4. Results and Discussion

4.1 Expression analysis of cGAS and STING in breast cancer

4.1.1 Expression analysis of cGAS and STING in different breast cancer cell lines

To understand the cross-talk of cGAS and STING in breast cancer, The expression of cGAS and STING were checked in breast cancer cell lines via real-time PCR and western blot. We selected different types of breast cancer cell lines like MCF-7, T47D, and ZR75 as (ER) estrogen receptor-expressing breast cancer cell lines also considered as hormone-responsive luminal type, MX-1 as ER non-expressing PR (progesterone expressing cell line) intermediate hormone-responsive and considered as baso-luminal type, BT-474 as HER2 expressing cell line and MDA-MB-231 as Triple-negative also consider as a basal type of breast cancer cell line. The analysis of mRNA level of cGAS by RT-qPCR (Fig-6, B) showed universal expression in both ER-positive (MCF-7, T-47D, ZR75) as well as negative breast cancer cell lines (MDA-MB-231, BT-474, and MX-1). In consonant rhyme with RT-qPCR data, western blotting showed the expression of cGAS protein in all selected breast cancer cells. Interestingly, we found that STING mRNA expression was lower in ER/PR positive breast cancer cell lines (MCF-7, T-47D, ZR75) compared to ER/PR negative breast cancer cell lines (MDA- MB- 231, BT-474, and MX-1) (Fig-6, A). In agreement with RNA expression, protein expression of STING was undetectable in ER-positive breast cancer cell lines (MCF-7, T-47D, and ZR75), whereas, its expression was predominantly high in ER-negative breast cancer cell lines (MDA- MB- 231, BT-474, MX-1) (Fig-6, D). cGAS expression was ubiquitously present in all cell lines (Fig,-6,C).

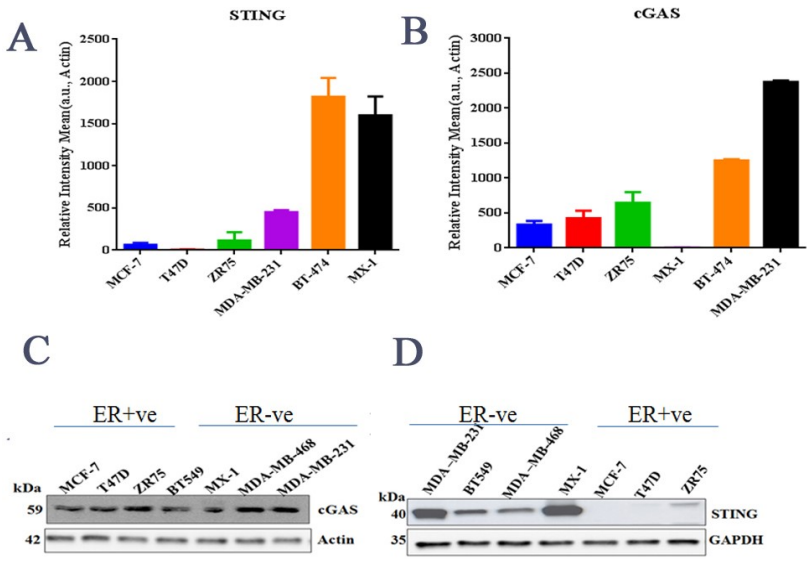

Figure 6 Expression pattern of cGAS and STING in different breast cancer cells

(A)Relative expression of STING in ER-positive (MCF-7, ZR75, T-47D) and ER-negative breast cancer cell lines (BT-474, MX-1 MDA MB 231) (B)Relative expression of cGAS in ER-positive (MCF-7, ZR75, T-47D) and ER-negative breast cancer cell lines (BT-474, MX-1 MDA MB 231) (C) Western blot analysis of cGAS and STING proteins in breast cancer cell (D) expression of STING in patient tissue western blot

4.1.2 Expression analysis of cGAS and STING in breast cancer patients

The expression of cGAS STING in cell lines studies was further extended to tumor tissues obtained from the breast cancer patient for a better understanding of the cross-talk of cGAS and STING. Western blot analysis was carried out to analyze protein levels and the expression of STING in tumor tissues, protein levels of STING were also high in all tumorous tissue as compared to the extra-tumoral tissue of the same patient (Fig- 7, C). To further validate the result, we check the expressing level correlation between the STING and ER (Estrogen receptor) utilizing the tumor data base interestingly the expression of STING was negatively correlated in all breast cancer types except the luminal type (Fig.-7, A). cGAS expressing also correlated with Estrogen receptor expression but no significant correlation was found (Fig-7, B)

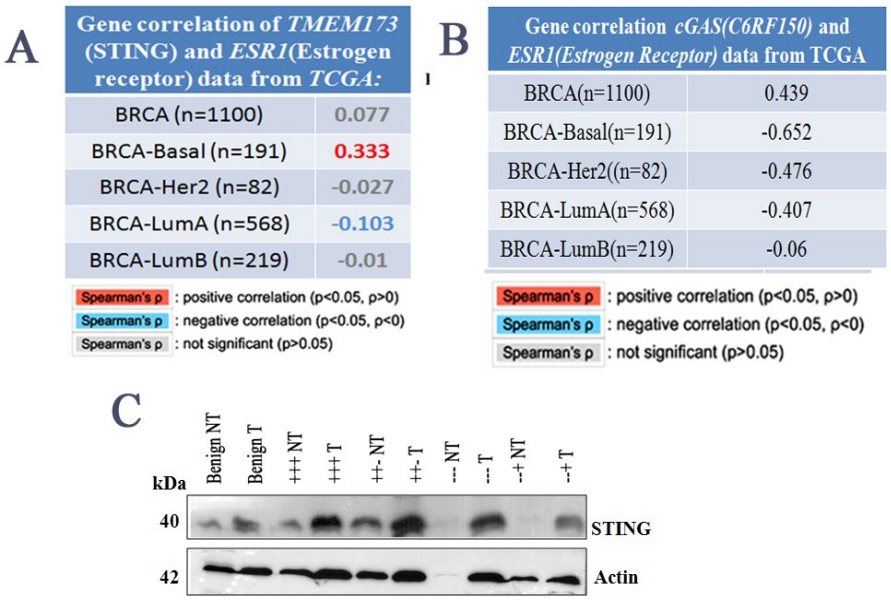

Figure 7 Expression pattern of cGAS and STING in different breast cancer patients

(A)Relative expression of STING negatively correlated with all types of breast cancer (B) Relative expression of cGAS negatively correlated with all types of breast cancer (C) Western blot analysis of STING proteins in patients' tissue

4.1.3 Discussion

As a result of the expression check, we conclude that the cGAS expression was uniform in all types of breast cancer while STING expression was significantly higher in the tumor as compared to non-tumor tissue. further, the deep correlation based on the cell line category MCF-7, T47D and ZR75 as ER-positive cell lines show low or undetectable levels in STING, While MX-1 as PR positive and BT474 and BT 549 as HER2 positive cell line has higher expression of STING and MDA-MB-231 and MDA-MB -468 as a triple-negative type of breast cancer cell line shows a higher level of STING expression. A comparable pattern was also observed that ER-positive cell lines have low and ER-negative cell lines have a higher expression [218]. However, the cGAS expression did not differ between ER-positive and ER-negative types of cell lines, and that is also supported via patient tumor data that expression of cGAS and ER do not correlate.

STING expression was overexpressed in ER-negative types of carcinogenic breast cancer cells as compared to ER-negative and non-tumor tissue. cGAS and STING play a crucial role in the activation of type -1 immune response. Expression STING higher in ER-negative type of breast cancer cell lines and patient tissue became a venerable target for the treatment of TNBC type of breast cancer. Moreover, we also understand the cross-talk of cGAS and STING in tumorigenesis in breast cancer

4.2 To study the crosstalk between cGAS and STING and its effect on tumorigenesis of breast cancer

4.2.1 DNA damage induces NF-κB activation in STING positive triple-negative breast cancer cells

DNA damaging agents acting on the genome of the rapidly proliferating cancer cells had been the preferred target for developing chemotherapeutic anti-tumor drugs. Doxorubicin, a topoisomerase inhibitor, stalls the replication fork causing toxic DSBs and cell death [219]. Doxorubicin is one of the most effective agents for the treatment of breast cancer however it cannot eliminate all the breast cancer cells at the late stage and may provide a survival advantage Hence, we used doxorubicin-induced stress to understand its implication in DNA damage-induced inflammation, immune-suppressive mechanisms, and cell death. We analyzed the expression of cGAS and STING using western blotting in breast cancer cells. We used ER-positive: MCF-7, T47D and ZR75, PR positive: MX-1, HER2 Positive: BT-549, and triple-negative: MDA-MB-468, MDA-MB-231 breast cancer cells. The 59 kDa band corresponding to cGAS was observed in all the breast cancer cell lines (Fig.-8, A). Western blotting showed that ER/PR positive cell lines: MCF-7, T47D, and ZR75 show low or undetectable STING expression, whereas HER2 positive: BT-549 and TNBC cell line: MDA-MB-468, MDA-MB-231 showed higher expression of STING (Fig-.8, B). Double-stranded breaks induced by DNA damaging agent lead to phosphorylation of Ser-139 residue of the histone variant H2AX, forming γH2AX, which is observed in different cell types and recruits proteins of DNA damage repair pathway. The detection of γH2AX has become an established marker of a double-stranded break during DNA damage[220]. Hence, we analyzed γH2AX in doxorubicin-treated breast cancer cells. We observed doxorubicin-induced upregulation of γH2AX in a time-dependent manner (Fig.-8, C). We further used MCF-7 as STING negative and MDA-MB-231 as STING expressing cell line for analysis of STING mediated NF-κB activation during DNA damage. MDA-MB-231 showed higher activation of the NF-κB pathway, whereas it remained at basal level in the MCF-7 cell line. DNA damage-induced NF-κB activity was further enhanced in MDA-MB-231 cells as compared to MCF-7 cells (Fig.-8, D). DNA damage-induced NF-κB activation may be essential for survival during genotoxic stress conditions [221], hence, we analyzed the role of cGAS/STING in NF-κB expression in different cell lines. The knockdown of cGAS and STING in MDA-MB-231 and MX-1 cell lines, cGAS knockdown showed no effect on NF-κB activation during DNA damage whereas STING knockdown inhibits NF-κB activation (Fig.-8, E, F). The

knockdown of cGAS and STING in MDA-MB-231 and MX-1 was confirmed by western blotting (Fig.-8, G, H). Nuclear translocation of p65-GFP was observed in doxorubicin-treated MDA-MB-231 (STING +ve cell line), whereas it remained in cytoplasm both in control and doxorubicin treated, MCF-7, (STING –ve cell line) (Fig.-8, K). We further confirmed the nucleus translocation of p65 by subcellular fractionation and western blotting. MDA-MB-231 and MDA-MB-468 show higher levels of p65 in the nucleus as compared to the MCF-7 STING negative cell line (Fig.-8, L, M). To confirm if STING was essential for NF- κB activation in MCF-7 (ER/PR +ve breast cancer cells), we overexpressed STING in MCF-7 and monitored NF-κB activation. The expression of STING in MCF-7 shows upregulation of NF-κB (Fig.-8, I, J). The evidence here suggests STING is highly expressed in triple-negative breast cancer cells as compared to ER/PR positive cells and is essential for NF-κB activation during DNA damage conditions.

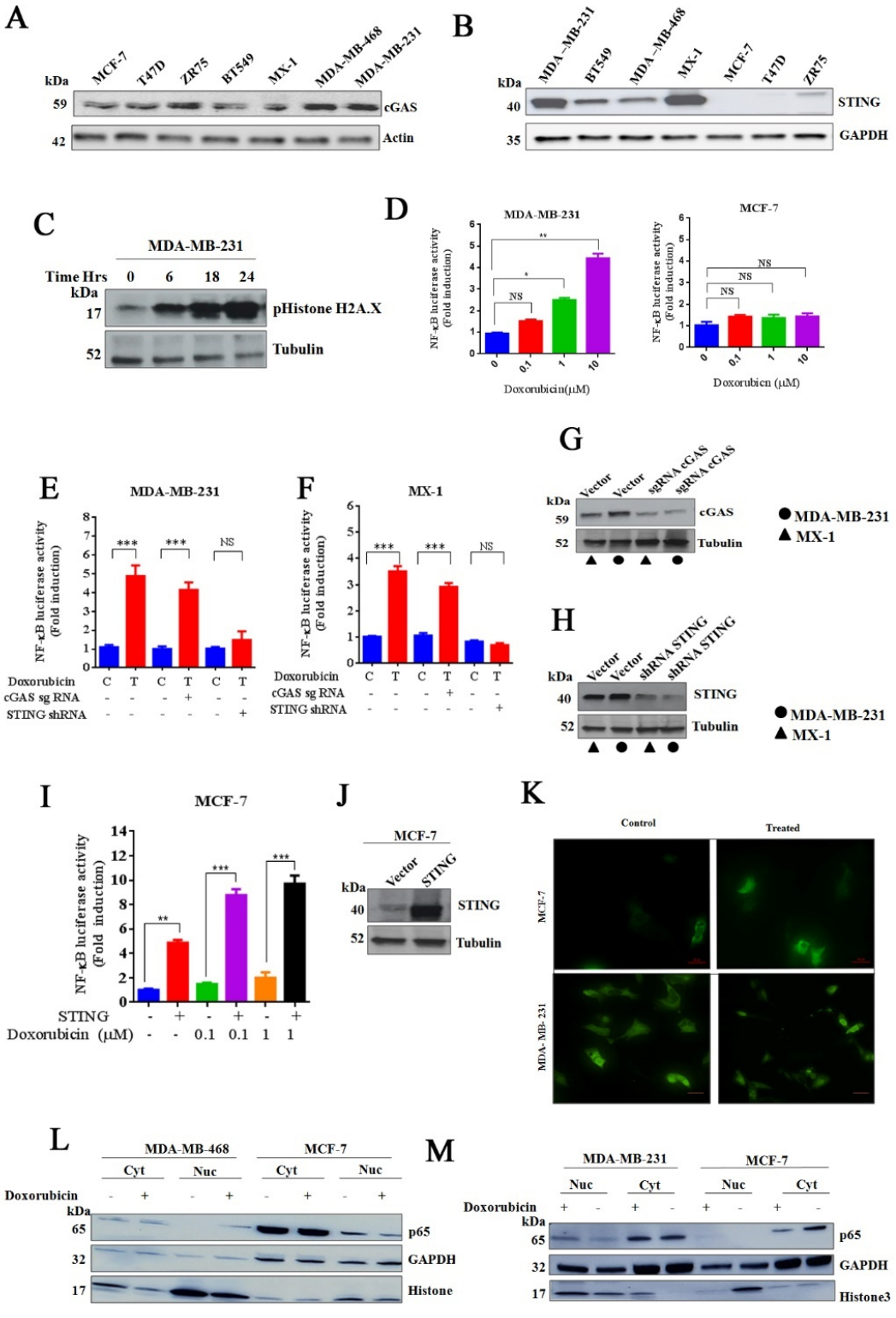
A
kDa
MCF-7
T47D
ZR75
BT549
MX-1
MDA-MB-468
MDA-MB-231
59
cGAS
42
Actin
B
kDa
MDA-MB-231
BT549
MDA-MB-468
MX-1
MCF-7
T47D
ZR75
40
STING
35
GAPDH
C
MDA-MB-231
Time Hrs 0 6 18 24
kDa
17
pHistone H2A.X
52
Tubulin
D
MDA-MB-231
MCF-7
NF-κB luciferase activity (Fold induction)
NS
Doxorubicin(μM)
Doxorubicn (μM)
E
MDA-MB-231
NF-κB luciferase activity (Fold induction)
***
NS
Doxorubicin C T C T C T
cGAS sg RNA - - - + - -
STING shRNA - - - - - +
F
MX-1
NF-κB luciferase activity (Fold induction)
***
NS
Doxorubicin C T C T C T
cGAS sg RNA - - - + - -
STING shRNA - - - - - +
G
kDa
Vector
Vector
sgRNA cGAS
sgRNA cGAS
59
cGAS
52
Tubulin
MDA-MB-231
MX-1
H
kDa
Vector
Vector
shRNA STING
shRNA STING
40
STING
52
Tubulin
MDA-MB-231
MX-1
I
MCF-7
NF-κB luciferase activity (Fold induction)
**
***
***
STING - + - + - +
Doxorubicin (μM) - - 0.1 0.1 1 1
J
MCF-7
kDa
Vector
STING
40
STING
52
Tubulin
K
Control
Treated
MCF-7
MDA-MB-231
L
MDA-MB-468
MCF-7
Cyt
Nuc
Cyt
Nuc
Doxorubicin - + - + - + - +
kDa
65
p65
32
GAPDH
17
Histone
M
MDA-MB-231
MCF-7
Nuc
Cyt
Nuc
Cyt
Doxorubicin + - + - + - + -
kDa
65
p65
32
GAPDH
17
Histone3

Figure 8 DNA damage induces NF-κB activation in STING-positive triple-negative breast cancer cells

Analysis of expression of cGAS and STING in breast cancer cells: Expression of cGAS and STING was analyzed by western blotting inMCF-7, T47D, ZR75 ER (+ve), MX-1 PR(+ve), BT549 HER2 (+ve), and MDA-MB-231, MDA-MB -468 as triple-negative cell lines (A) and for STING (B).Doxorubicin-induced activation of phosho- Histone H2A.X in a time-dependent manner: MDA-MB-231 cells were treated with doxorubicin, cell lysate was collected at different time points and western blot was performed (C) Analysis of STING mediated NF-κB activation by luciferase assay: MCF-7 and MDA-MB-231 were transfected with 5X-NF-κB-Luc and treated with doxorubicin for 24 hrs and luciferase activity was analyzed using DLR assay(D).Effect of cGAS and STING knockdown on NF-κB activation: Sequentially cGAS and STING knockdown in MDA-MB-231 and MX-1, cells were transfected with 5X-NF-κB-Luc and treated with doxorubicin for 24 hrs and luciferase activity was analyzed using DLR assay(E&F). Representative western blot for knockdown of cGAS and STING in MDA-MB-231 and MX-1(G&H). Effect of STING overexpression on NF-κB activation in MCF-7 cells: STING was overexpressed in MCF-7 and cells were transfected with 5X-NF-κB-Luc and treated with doxorubicin for 24 hrs and luciferase activity was analyzed using DLR assay (I) and representative western blot image for overexpression of STING in MCF-7 (J) Analysis of p65 translocation during DNA damage in breast cancer cells: MCF-7 and MDA-MB-231 were transfected with p65-GFP and treated with doxorubicin for 6 Hrs and translocation of p65 was analyzed under a fluorescence microscope (K). Nuclear translocation of p65 to the nucleus by western blotting: MCF-7 and MDA-MB-231 and MDA-MB-468 cells were treated with doxorubicin for 6 Hrs and subcellular fractions were prepared and analyzed by western blotting using specific antibodies (L&M).

4.2.2 STING mediated NF-κB activation induces IL-6 expression in triple-negative breast cancer cells in DNA damage conditions:

The activation of NF-κB in breast cancer cells in the tumor microenvironment leads to the expression of several cytokines which may amplify survival signals and leads to resistance to cell death during stress conditions[222][223]. Hence, we analyzed the possible role of STING-mediated differential NF-κB activation modulating the expression of IL-6, a key

cytokine that is essential for survival and drug resistance in breast cancer cells [224]. Different subtypes of breast cancer cells were treated with doxorubicin and analyzed for IL-6 secretion in media by ELISA. Interestingly, MCF-7, T47D, and ZR75 (ER/PR positive cells) show basal IL-6 levels whereas MX-1, BT549, MDA-MB-231, and MDA-MB-468 (Triple-negative cells) showed significantly elevated IL-6 levels (Fig.-9, A). The expression and secretion of IL-6 increased with time in presence of doxorubicin in MDA-MB-231(STING +ve cell line) as compared to T47D (STING –ve cell line) suggesting that STING is essential for the expression of IL-6 (Fig.-9, B). IL-6 binds to its cognate receptor complex IL6R/gp130 and activates downstream Janus kinases (JAKs), which activate downstream STAT3 through phosphorylation of Tyrosine 705 [225]. We investigated if IL-6 differentially activates a downstream pathway in the STING high/low breast cancer cells. We treated the cells with doxorubicin and monitored pSTAT3Y705 phosphorylation by western blotting using a phospo-STAT3-specific antibody. The phosphorylation of STAT3 was significantly enhanced in MDA -MB-231, STING positive cells whereas was not detected in T47D as STING negative cell line (Fig.-9, C). Previous reports suggested that DNA damage-induced IL-6 may activate downstream JAK-STAT pathway STAT3 via an autocrine mechanism [59]. STING was knockdown both in MDA-MB-231 and MX-1 and monitored pSTAT3 Y705 using a specific antibody. Interestingly. pSTAT3 Y705 levels were elevated in MDA-MB-231 and MX-1 control cells and were undetectable in STING knockdown conditions (Fig.-9, D, E). The knockdown of STING expression was also confirmed in both cell lines (Fig.-9, F, G). The evidence here suggests DNA damage induces STING-mediated IL-6 expression and autocrine activation of the downstream STAT3 pathway in triple-negative breast cancer cells.

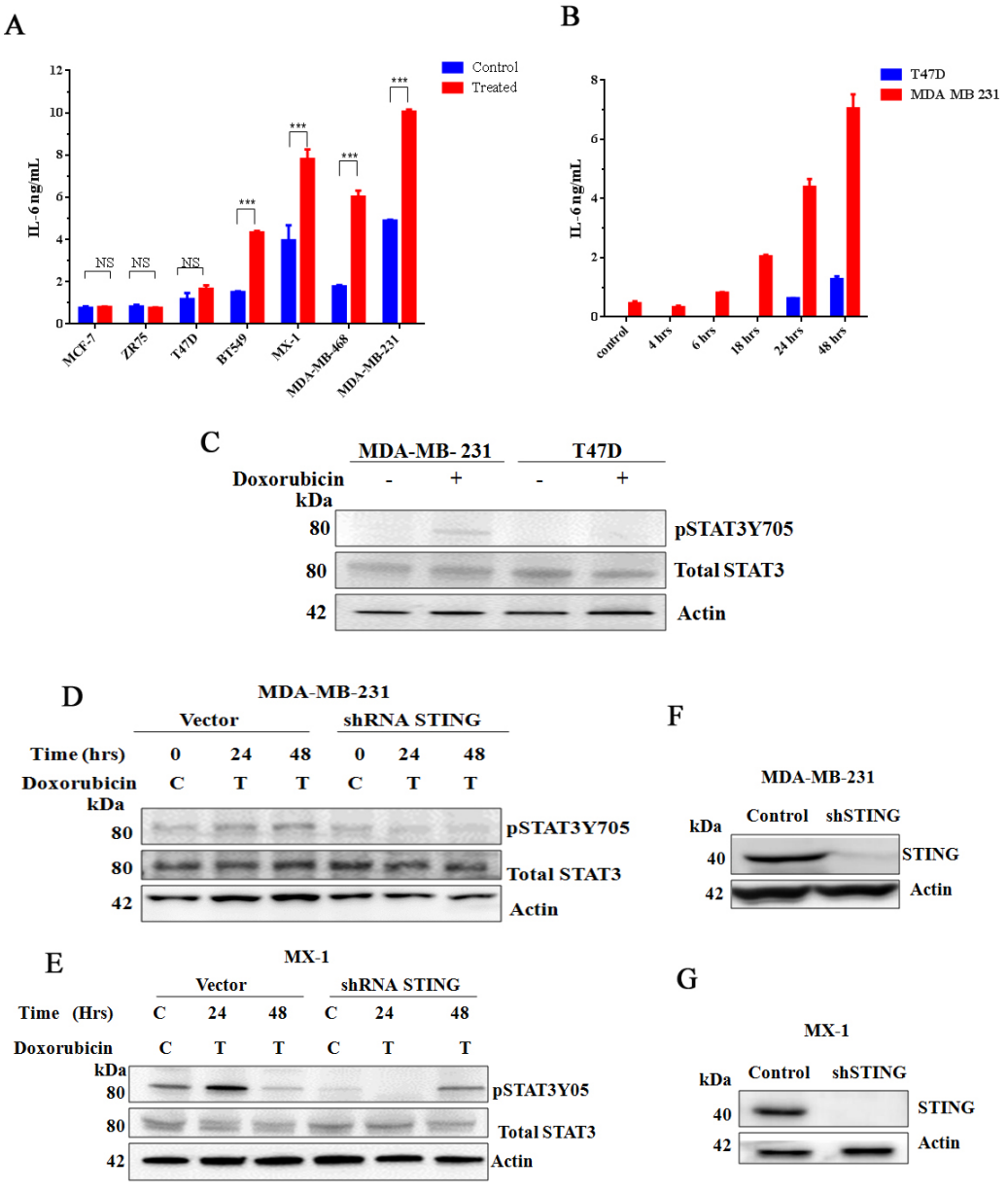

Figure 9 STING mediated NF-κB induces IL-6 expression in STING-positive triple-negative breast cancer cells

Analysis of IL-6 during DNA damage: Breast cancer cell lines treated with doxorubicin and IL-6 levels were analyzed in media supernatants by ELISA (A). Analysis of IL-6time-dependent during DNA damage: T47D and MDA-MB-231 cell lines were treated with doxorubicin and IL-6 was analyzed by ELISA (B). Analysis of pSTAT3Y705 during DNA damage: T47D and MDA-MB-231 cell lines were treated with doxorubicin for 24 hrs and

pSTAT3Y705 levels were analyzed via western blotting (C).Effect of STING knockdown on level pSTAT3Y705 during DNA damage: MDA-MB-231 and MX-1 were transfected with shRNA of STING and treated with doxorubicin for 24 and 48 hrs and levels of pSTAT3Y705 were analyzed by western blotting (D).Analysis of STING knockdown: Western blot was performed to show the level of STING knockdown in MDA-MB-231(F) and MX-1 (G)breast cancer cell lines.

4.2.3 The knockdown of STING sensitizes breast cancer cells to genotoxic stress and inhibits clonogenicity:

The activation of the IL-6/STAT3/NF-κB pro-inflammatory circuit in tumor cells, other cell types in TME, and cancer-associated fibroblasts isolated from breast cancer patients play a critical role in tumor progression [223]. We investigated if STING-mediated IL-6/STAT3/NF-κB activation is important for the resistance to genotoxic drugs in breast cancer cells. We knockdown STING in MDA-MB-231 and MX-1 and treated them with doxorubicin and monitored cell viability. Knockdown of STING sensitized both MDA-MB-231 and MX-1 cells to doxorubicin (Fig.-10, A, C). IC_{50} of doxorubicin shifted 0.126 µM to 0.066 µM in STING knockdown in MDA-MB-231, a similar IC_{50} shift was also observed in MX-1 with 0.07 µM to 0.03µMin STING knockdown conditions (Fig.-10, B, D). We generated a stable knockdown of STING in MDA-MB-231(shSTING) and monitored its ability to generate a 3D spheroid. Further MDA-MB-231 form a strong and dense spheroid whereas MDA-MB-231(shSTING) formed a dispersed spheroid and showed inhibition of spheroid formation in the presence of doxorubicin (Fig.-10, E). We also analyzed the sensitivity of the MDA-MB-231(shSTING) to doxorubicin by analyzing the cell viability and observed that MDA-MB-231(shSTING) cells were more sensitive and showed decreased viability as compared to control MDA-MB-231 cells (Fig.-10, F). We also analyzed the clonogenic abilities of both MDA-MB-231 cells and BT-549 cells in STING knockdown cells. Interestingly reduced STING levels reduce the clonogenic abilities of both MDA- MB-231 (Fig.-10, G) and BT-549 cells (Fig.10, H)

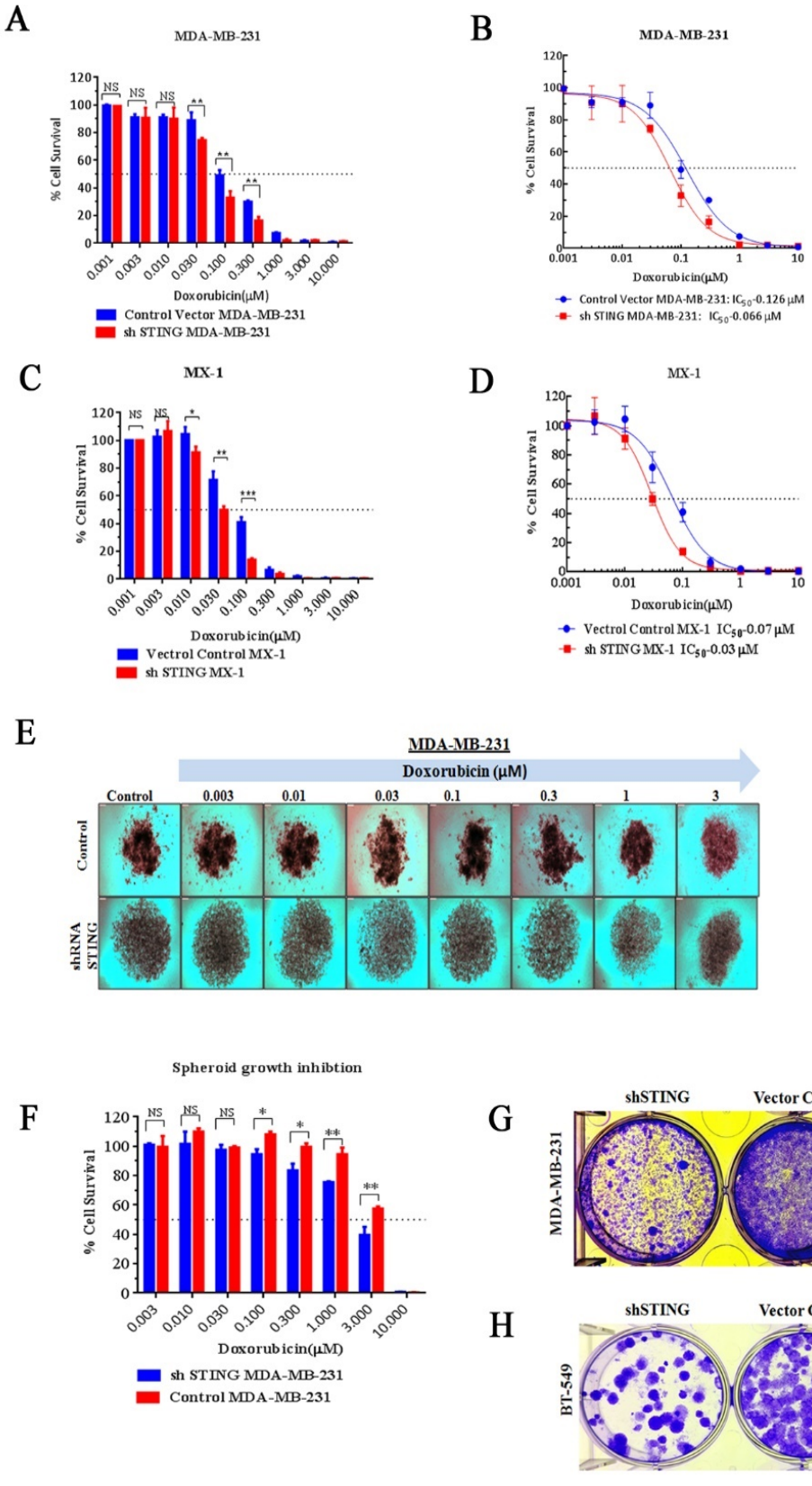
A
MDA-MB-231
% Cell Survival
Doxorubicin(μM)
Control Vector MDA-MB-231
sh STING MDA-MB-231
B
MDA-MB-231
% Cell Survival
Doxorubicin(μM)
Control Vector MDA-MB-231: IC50-0.126 μM
sh STING MDA-MB-231: IC50-0.066 μM
C
MX-1
% Cell Survival
Doxorubicin(μM)
Vectrol Control MX-1
sh STING MX-1
D
MX-1
% Cell Survival
Doxorubicin(μM)
Vectrol Control MX-1 IC50-0.07 μM
sh STING MX-1 IC50-0.03 μM
E
MDA-MB-231
Doxorubicin (μM)
Control
0.003
0.01
0.03
0.1
0.3
1
3
Control
shRNA STING
F
Spheroid growth inhibtion
% Cell Survival
Doxorubicin(μM)
sh STING MDA-MB-231
Control MDA-MB-231
G
shSTING
Vector Control
MDA-MB-231
H
shSTING
Vector Control
BT-549

Figure 10 The knockdown of STING sensitizes breast cancer cells to doxorubicin

Effect of STING knockdown on cell survival in presence of doxorubicin: MDA-MB-231 and MX-1 were transfected with STING shRNA and treated with different concentrations of doxorubicin for 4 days and % Viability measured (A)&(C). Effect of knockdown of STING on growth in presence of doxorubicin and IC_{50} was calculated (B) & (D) Effect of doxorubicin on 3D spheroid condition: MDA-MB-231 and MDA-MB-231 (shSTING) cells were seeded to form spheroid as described in the method section, spheroid generation at different concentrations of doxorubicin was analyzed after 7 days (E). Cell viability is plotted in Bar graph (F) Effect of STING knockdown on clonogenicity: MDA-MB-231 and BT549 were transfected with STING shRNA and colony formation assay was performed (G)(H) STING mediated IL-6 induction enhances PD-L1 expression during DNA damage in triple-negative breast cancer cells

4.2.4 STING-mediated IL-6 induction enhances PD-L1 expression during DNA damage in triple-negative breast cancer cells

Genotoxic stress may induce the release of nuclear DNA in the cytosol and the formation of micronuclei which activate the STING-mediated NF-κB pathway further modulating the survival pathway and immune suppression mechanism by regulating PD-L1[226][54]. We analyzed if STING modulates the immune suppressive mechanisms in breast cancer cells in the presence of doxorubicin. Interestingly, MDA-MB-231 cells treated with doxorubicin showed an enhanced level of 45 kDa band corresponding to PD-L1 (Fig.-11, A). As we observed above doxorubicin-induced IL-6 expression and release hence we hypothesized that STING regulated IL-6-STAT3 pathway may regulate the expression of PD-L1. Hence, we treated MDA-MB-231 cells with IL-6 and monitored the expression of PD-L1 by western blotting. The western blotting showed that PD-L1 expression was directly proportional to the dosage of IL-6 (Fig.-11, B). To confirm if the expression of PD-L1 is mediated through STING/IL-6/STAT3 pathway, STING was knockdown in MDA-MB-231 and monitored PD-L1 expression. The knockdown of STING in MDA-MB-231 cells decreased PD-L1 expression (Fig.-11, C). We used HJC0152, an Anti-helminthic drug that inhibits STAT3 phosphorylation and hence inhibits the STAT3 pathway [227]. MDA-MB-231 cells treated with HJC0152 and showed a decreased level of PD-L1 (Fig.-11, D). Flowcytometry analysis also showed decreased surface expression of PD-L1 in STING knockdown MDA-MB-231 (Fig.5.2.4, E), as monitored by mean

fluorescence Intensity (Fig.-11, F). These experiments suggest that STING-mediated IL-6 production during DNA damage conditions induces PD-L1 expression which may be one of the immune escape and suppression mechanisms in breast cancer cells during DNA damage. Overexpression of PD-L1 on cancer cells helps to escape the cell-mediated immune response, hence we tested further inhibiting PD-L1/PD1 interaction using an anti-PD-L1 antibody.MDA-MB-231 (control) and MDA-MB-231(shRNA STING) knockdown cells were incubated with PD-L1 antibody and activated lymphocytes. The activated lymphocytes were able to induce immune cell death in anti-PD-L1 treated cells. Interestingly MDA-MB-231(shRNA STING) cells with lymphocytes show a similar level of activated PBMCs mediated cell death. This further supports our hypothesis that STING expression in triple-negative breast cancer provides an immune escape mechanism during DNA damage conditions. The stable cell line MDA-MB-231(STING shRNA) line showed decreased expression of PD-L1 as compared to the control MDA-MB-231(WT) parent cell line. Downregulation of PD-L1 show enhanced T cell activity in CD4 and CD8 T cells reflected by both higher cell death of target cells. Giemsa-stained surface area plotted using ImageJ (Fig.-11,4G) and representative image of Giemsa stain. (Fig.-11, H) Significantly higher amount of IFN-γ production by both CD8 and CD4 T cells in response to sh STING target cells as compared to WT target cells at 1:16 target: effector ratio as assessed by intracellular staining and flow cytometry (Fig.4 I, J). Atezolizumab, FDA-approved PD-L1 inhibitor antibody was used as a positive control for the suppressive effect.

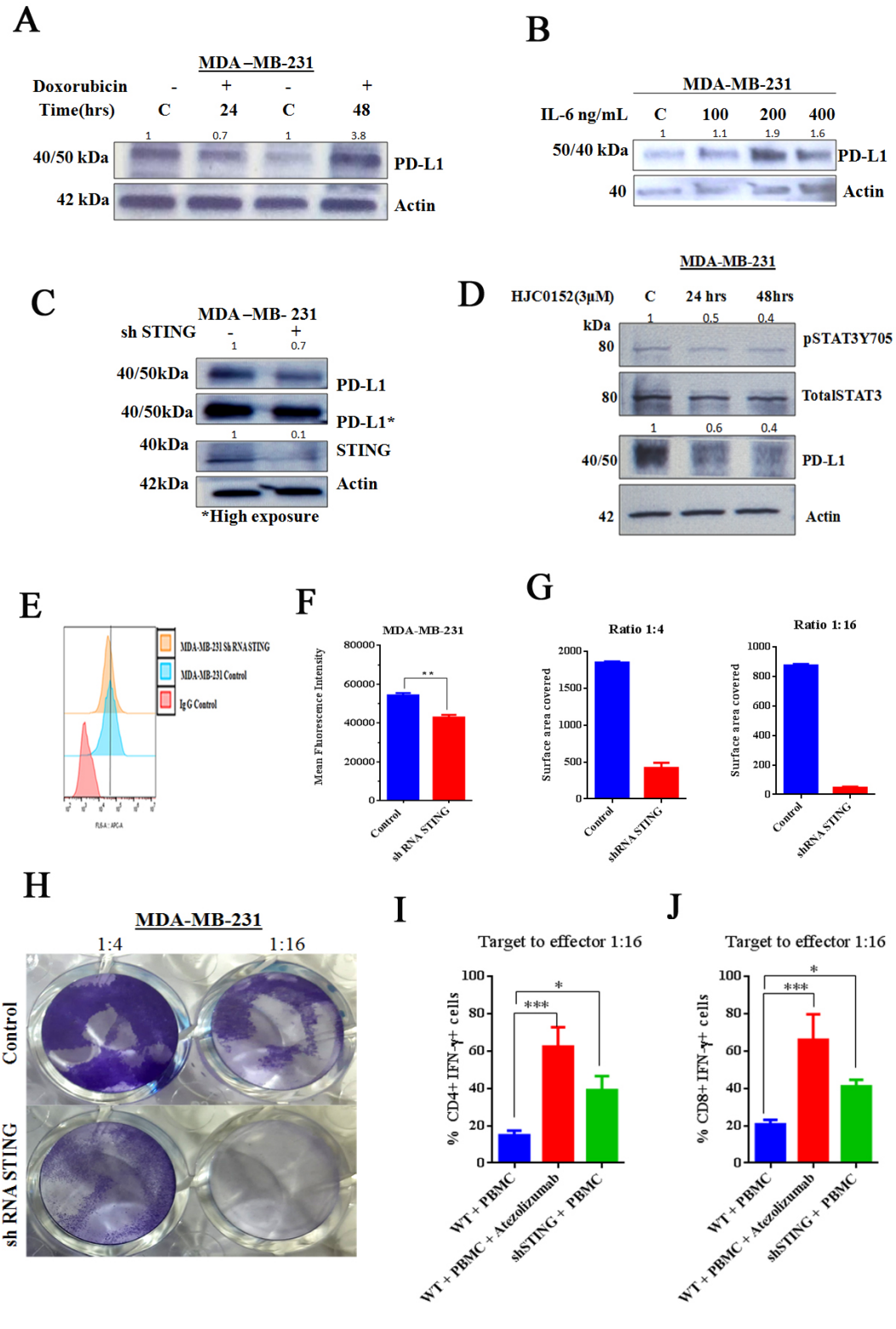
A
MDA –MB-231
Doxorubicin - + - +
Time(hrs) C 24 C 48
1 0.7 1 3.8
40/50 kDa
PD-L1
42 kDa
Actin
B
MDA-MB-231
IL-6 ng/mL C 100 200 400
1 1.1 1.9 1.6
50/40 kDa
PD-L1
40
Actin
C
MDA –MB- 231
sh STING - +
1 0.7
40/50kDa
PD-L1
40/50kDa
PD-L1*
1 0.1
40kDa
STING
42kDa
Actin
*High exposure
D
MDA-MB-231
HJC0152(3μM) C 24 hrs 48hrs
kDa
1 0.5 0.4
80
pSTAT3Y705
80
TotalSTAT3
1 0.6 0.4
40/50
PD-L1
42
Actin
E
MDA-MB-231 Sh RNA STING
MDA-MB-231 Control
Ig G Control
F
MDA-MB-231
Mean Fluorescence Intensity
80000
60000
40000
20000
0
**
Control
sh RNA STING
G
Ratio 1:4
Surface area covered
2000
1500
1000
500
0
Control
shRNA STING
Ratio 1:16
Surface area covered
1000
800
600
400
200
0
Control
shRNA STING
H
MDA-MB-231
1:4
1:16
Control
sh RNA STING
I
Target to effector 1:16
% CD4+ IFN-γ+ cells
100
80
60
40
20
0
*
***
WT + PBMC
WT + PBMC + Atezolizumab
shSTING + PBMC
J
Target to effector 1:16
% CD8+ IFN-γ+ cells
100
80
60
40
20
0
*
***
WT + PBMC
WT + PBMC + Atezolizumab
shSTING + PBMC

Figure 11 STING up-regulates IL-6 mediated PD-L1 expression during DNA Damage and suppresses immune cell death

DNA damage induces PD-L1 expression: MDA-MB-231 was treated with doxorubicin for 24 hrs and 48 hrs and western blotting was performed for the expression of PD-L1(A). IL-6 induces PD-L1 expression: MDA-MB-231 was treated with different concentrations of IL-6 for 24 hrs and PD-L1 expression was analyzed by western blotting(B). Effect of STING knockdown on PD-L1 expression: MDA-MB-231 was transfected with shRNA of STING and the expression PD-L1 was analyzed via western blotting(C).Effect of HJC0152 on the expression of pSTAT3 and PD-L1: MDA-MB-231 cells were treated with HJC0152 (STAT3 Inhibitor) for 24 hrs and expression of total STAT3,pSTAT3 Y705, and expression of PD-L1 was analyzed via western blotting(D).Surface PD-L1 expression in STING knockdown condition: PD-L1 levels in MDA-MB-231, sh RNA STING, and MDA-MB-231 (wt) cell lines were analyzed for by flow cytometry (E, F) T cell-mediated immune response inhibition in PD-L1 overexpression and reduction condition: T cell cytotoxicity test by colony formation assay. MDA-MB-231 and MDA-MB-231-shRNA-STING cells were co-cultured with PBMCs (targeted cells: effectors cells =1:4, 1:16) in presence of PD-L1 Ab in 24-well plates for 4 days and colonies were visualized by Giemsa staining(G). Survival relative to control is shown (H)&(I) Interferon response γ in T cell activation: The activation of CD8 and CD4 cells as IFN-γ in presence of anti-PD-L1 antibody (Atezolizumab) and in shSTING stable cell line (H)(I)

4.2.5 STAT3 inhibitor, HJC0152and doxorubicin act synergistically in breast cancer cells to inhibit cell death

STAT3, a transcription factor, is hyper-activated in many tumor cells including breast cancer [228], and its inhibition has been proposed as a possible drug target in breast cancer[59], [229]. Hence, we analyzed the combinatorial cytotoxic potential of HJC0152, STAT3 inhibitor and doxorubicin against MDA-MB-231 and MX-1 cell lines. Interestingly combination of both the drug shows a synergistic effect in growth inhibition (Fig.-12, A, B), Microscopic analysis also showed enhanced cell death in presence of combinatorial treatment of doxorubicin and HJC0152 (Fig.-12,E). Caspase3/7 activity also increased in MDA-MB-231 and MX-1, STING +ve cell lines, in presence of both HJC0152 and doxorubicin as compared to individual treatments (Fig.-12, C, D). We also checked the PARP cleavage as a marker of apoptosis in these conditions via western

blotting. The band of 86 kDa corresponding to cleaved PARP cleavage increased significantly in combinatorial treatment conditions as compared to individual treatments (Fig.12, F, G)

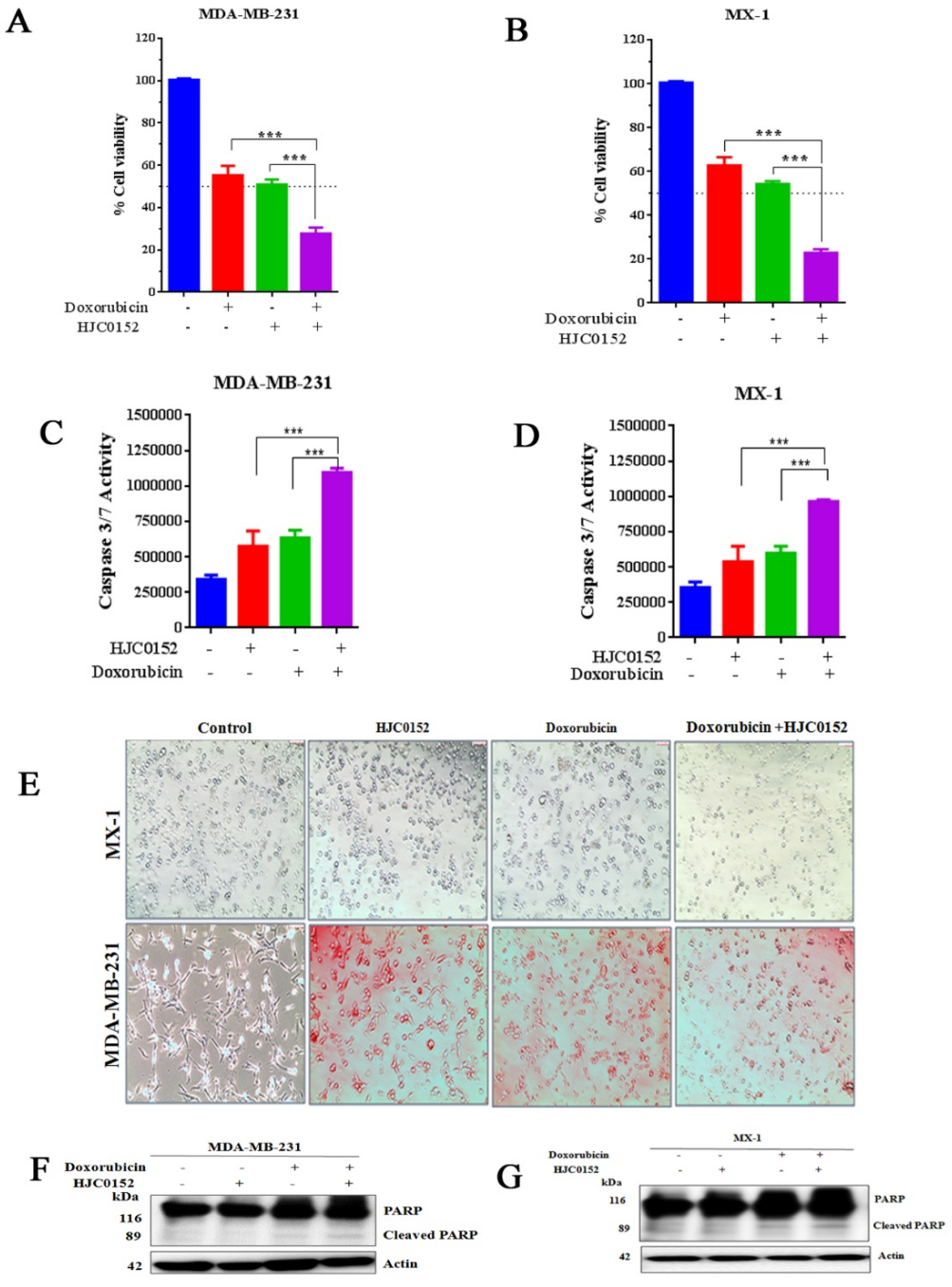

Figure 12 STAT3 inhibitor, HJC0152 and doxorubicin act synergistically in breast cancer cells to inhibit cell death

Effect of combinatorial treatment of STAT3 inhibitor and doxorubicin on cell viability: MDA-MB-231 and MX-inhibition: MDA-MB-231 and MX-1 treated with doxorubicin, HJC0152 and combinations of both and % cell viability was analyzed(A)&(B). Effect of combinatorial treatment of STAT3inhibitor and doxorubicin on capase3/7 activity: MDA-MB-231 and MX-1 treated with 1µM doxorubicin, 3 µM of HJC0152 and combinations of both drugs and Caspase3/7 activity (C)&(D). Effect of combinatorial treatment of STAT3 inhibitor and doxorubicin on growth: MDA-MB-231 and MX-1 were treated with 1µM doxorubicin, 3 µM of HJC0152 and combinations and cells were analyzed using a microscope (E). Effect of combinatorial treatment of STAT3 inhibitor and doxorubicin on PARP cleavage: Cells were treated with 1µM doxorubicin,3 µM of HJC0152 and combinations of both for 24 hrs and cleaved PARP measured using western blotting(F)(G).

4.2.6 STING expression positively correlates with IL6 and PD-L1 expression and high STING expression in chemotherapy shows poor survival

Tumor Immune Estimation Resource (TIMER) is a database of more than 32 cancer and is a web-based server to analyze the correlation between gene expression and immune cell infiltration. It also provides the gene expression and its correlation with breast cancer type and progression of the tumor[230]. We used the TIMER database to compare the mRNA expression of different genes such as STING and IL6 and PD-L1genes in different breast cancer subtypes[217]. Interestingly, the expression of STING (TMEM173) positively correlates with CD274(PD-L1) and IL6 positively correlates with CD274(PD-L1) levels in invasive carcinoma, Basal, luminal, HER2 type breast cancer (Fig.-13, A). We also analyzed the correlation of the STING(TMEM173) gene with the expression of three genes as PD-L1, ESR1(Estrogen receptor) and IL6 in breast cancer. TMEM173(STING) positively correlated for PD-L1, and IL6. Further TMEM173(STING) negatively correlated with ESR1 (Estrogen receptor) in invasive carcinoma, Basal, luminal, HER2 type breast cancer(Fig-13, B).This data is in consonance with our *in-vitro* data higher expression of STING in ER-negative cell lines.

We analyzed the Kaplan- Meier survival curves of patients having STING expression using a web-based curator[216]. Patients having a higher expression of STING show poor

outcomes in terms of survival as {HR= 1.54(0.93-2.53) log Rank p=0.089} during chemotherapy. Similarly, in the second database, TMEM173 (STING) expression worsens survival as the{HR=1.41(0.92-2.49) log Rank p=0.1}. During chemotherapy, low expression of STING (TMEM173)(represented by black line) showed better survival where as higher expression of STING(TMEM173) (represented by red line) (Fig-13, C D) worsened the survival.

A

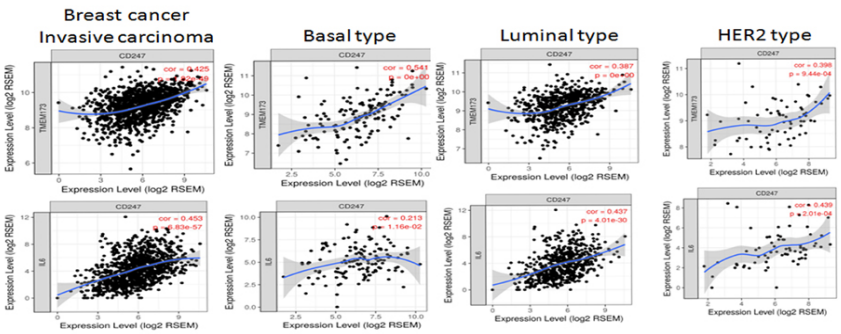

B

Spearman's ρ : positive correlation (p<0.05, ρ>0)
Spearman's ρ : negative correlation (p<0.05, ρ<0)
Spearman's ρ : not significant (p>0.05)

cancer	CD274	ESR1	IL6
BRCA (n=1100)	0.421	0.077	0.337
BRCA-Basal (n=191)	0.522	0.333	0.388
BRCA-Her2 (n=82)	0.365	-0.027	0.294
BRCA-LumA (n=568)	0.468	-0.103	0.388
BRCA-LumB (n=219)	0.461	-0.01	0.219

C

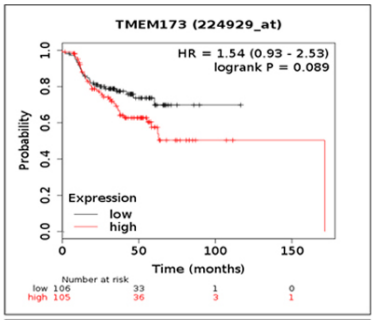

Upper quartile survival	
Low expression cohort (months)	High expression cohort (months)
46.49	27

D

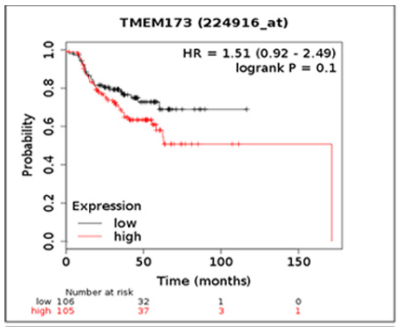

Upper quartile survival	
Low expression cohort (months)	High expression cohort (months)
42.05	25.76

Figure 13 STING expression positively correlates with IL-6 and PD-L1 and High Expression of STING in chemotherapy shows the poor outcome

Gene expression correlation: Analysis using TIMER database between STING and PD-L1(CD247) and IL-6 and PL-1(CD247) in Invasive Carcinoma, Basal Type, Luminal Type, HER2 type of Breast cancer(A). Gene expression correlation: Positive or negative correlation in subtypes of breast cancer for CD274, ESR1 and IL6 using TIMER database(B) Kaplan Meier survival analysis: Plot for TMEM173in breast cancer patients' survival with chemotherapy (C)&(D).

4.2.7 Discussion:

The tumor microenvironment of solid tumors is complex and the constant interaction of tumor cells with immune cells determines the progression of tumors. The tumor cells are the major focus of such interactions which evolve and retain the expression of the key genes required for the immune evasion and cell survival pathway during stress conditions. Triple-negative breast cancer cells are highly proliferative and show a high level of chromosomal instability [231]and retain the expression of key proteins of innate immune pathways: cytoplasmic sensors like cGAS and STING, which sense DNA and can modulate the cell survival pathways in stress conditions[50]. In the current study, we demonstrate that STING activates IL-6 mediated STAT3 pathway during genotoxic stress which inhibits immune suppression via enhancing PD-L1 in malignant triple-negative breast cancer cells. This helps to evade the immune response and is negatively correlated with a patient's survival.

The activation of cGAS and STING pathways in tumor cells and immune cells recruited in the tumor microenvironment had been of major interest as it may help to modulate tumor intrinsic cell survival and death pathways[232]. Interestingly the expression of STING was expressed at the higher level in TNBC and ER-negative type of cells (MDA-MB-231, MX-1, BT549, MDA-MB-468) and is low or undetectable in ER-positive cell lines like MCF-7, T47D, and ZR75.As we observed here that different breast cancer cell lines show a similar expression level of cGAS whereas STING is only retained in triple-negative breast cancer cells which may provide a survival advantage specifically to triple-negative breast cancer cells. This agrees with the previous observation from our lab and others[50][58]. Interestingly we observed that genotoxic stress conditions cGAS was dispensable for NF-κB activation whereas STING was indispensable for NF-κB activation

in triple-negative breast cancer cells. The implication of NF-κB pathway in the survival pathway during genotoxic stress conditions can be either pro and anti-apoptotic depending upon the breast cancer cells subtypes and growth stage. Previously we demonstrated that enforced STING expression in ER/PR positive cells shows activation of caspase-8 mediated cell death[218]. Hence this probably explains the loss of STING in early phase triple-positive breast cancer cells. The response to NF-κB during genotoxic stress conditions may be dependent upon the dosage and duration of stress induction in cells.

In breast cancer there is limited targeted therapy available for TNBC and chemotherapy is widely used for the treatment of TNBC[233]. The evidence, here suggests that doxorubicin which induces genotoxic stress conditions in highly proliferative cancer cells shows activation of STING-mediated NF-κB pathway and induces expression of IL-6 and STAT3 pathway in triple-negative breast cancer cells. This is in consonance with earlier observations where highly proliferative breast cancer cells show high CIN leading to the formation of micronuclei sensed by cGAS/STING which activates the non-canonical STING pathway that induces NF-κB and cell survival[50]. In the current study, we observed that DNA damage-induced alternate STING pathway of NF-κB activation in triple-negative breast cancer cells where cGAS showed no major role. This is in agreement with previous observations where DNA damage-induced alternate/ pathway of NF-κB activation rather than IFN pathway where STING binds to DNA binding protein IFI16 along with DNA damage response factors ATM and PARP-1 which forms an alternative STING signaling complex that includes the tumor suppressor p53 and the E3 ubiquitin ligase TRAF6[54]. The evidence here suggests the DNA damage activates STING-mediated alternate NF-κB activation and further role of this pathway in cell survival and immune evasion and immune cell death was explored. It will be also interesting to investigate the assembly of alternate signaling complexes and downstream co-operativity of p53 and p65 during DNA damage and their role in tumor progression.

During DNA damage, STING induced the expression of IL-6 which binds to its cognate receptor leading to the activation of phosphorylation of tyrosine (705) residue of STAT3[59], suggesting the activation of the STING-mediated IL-6/STAT3 pathway in triple-negative breast cancer cells during genotoxic stress conditions. It is known that IL6/STAT3 signaling plays a critical role in tumor progression in many solid tumor types

by inducing epithelial-to-mesenchymal transition (EMT) and angiogenesis[234]. Therefore IL6/STAT3 pathway is an attractive drug target in different solid tumors including breast cancer. Several approaches to target this pathway in different cancer are being pursued at different clinical stages. This includes the upstream targeting of JAKs and direct targeting of STAT3 phosphorylation and activation[229]. We investigated if the inhibition of the STAT3 pathway under genotoxic stress conditions sensitizes the ER-negative breast cancer cells to cell death. Niclosamide, a potent STAT3 inhibitor, by suppressing STAT3 phosphorylation at Tyr705 in adrenocortical carcinoma and prostate cancer [30]. HJC0152 an improved derivative of niclosamide and a potent inhibitor of STAT3 activation was used in the further study[63]. The evidence here suggests the combinatorial treatment of HJC0152 and doxorubicin sensitizes the breast cancer cells at a low dosage and HJC0152and shows synergistic growth inhibition of MDA-MB-231 and MX-1 STING expressing cell line. Hence it may be further interesting to explore the potential of the combinatorial therapeutic regimen of STAT3 inhibitors and genotoxic drugs which may work at low dosages and hence may avoid side effects.

DNA damage or high chromosomal instability as observed in highly malignant breast cancer cells shows immune evasion suggesting the important role of DNA damage-induced activation of the STING pathway. Here we demonstrated DNA damage induces PD-L1 expression in STING-negative triple-negative breast cancer cells. This is also in consonance with a previous report where DNA damage is known to induce PD-L1 where TBK1 had been shown to enhance the PD-L1 in tumor cells[235][200]. The STAT3 pathway is closely associated with PD-L1, a major blocker for T cell-mediated immune suppression mechanism in the tumor [236][237]. Our experiment clearly shows that down-regulation of STING sensitizes to immune cell death mediated by activated lymphocytes suggesting STING is a central regulator of resistance to immune cell death in triple-negative metastatic breast cancer cells during DNA damage conditions.

The activation of the STING-mediated survival pathway during DNA damage and further expression of PD-L1 suggest immune escape mechanisms. Hence, we analyzed different TCGA and other databases which strongly show that STING positively correlated with IL-6 and show poor survival outcomes. This strongly suggests that in triple-negative breast cancer patients this is one of the important drug resistance and immune escape mechanisms hence needs to be considered during chemotherapy. Further, we suggest that

combination therapy of DNA damaging agent and STAT3 inhibitor may act synergistically in the clinical condition to induce immune cell death in STING-expressing metastasis tumor cells. This needs further study to develop this combinatorial regimen and its possible analysis in a different model system for exploiting the STING pathway for clinical therapeutic in metastatic triple-negative breast cancer.

4.3 To study of the cGAS-STING pathway in anticancer therapy

4.3.1 c-di AMP induces STING-mediated IFN pathway in breast cancer cell lines:

We investigated if c-di-AMP can activate the STING pathway in breast cancer cells and modulate the IFN pathway. Firstly, we monitored the expression of STING in ER-positive and negative breast cancer cells. The analysis of transcript level of cGAS by RT-qPCR (Fig.-14, B) showed ubiquitous expression in both ER-positive (MCF-7, T-47D, ZR75) as well as negative breast cancer cell lines (MDA- MB- 231, BT-474 and MX-1). In consonance with RT-qPCR data, western blotting showed the expression of cGAS protein in all selected breast cancer cells. Interestingly, we found that STING mRNA expression was lower in ER-positive breast cancer cell lines (MCF-7, T-47D, ZR75) compared to ER-negative breast cancer cell lines (MDA- MB- 231, BT-474, and MX-1) (Fig.-14, A). Gene expression correlation *r* value represented in a different color in different types of breast cancer (Fig.-14, C). In agreement with RNA expression, protein expression of STING was undetectable in ER-positive breast cancer cell lines (MCF-7, T-47D, and ZR75), whereas, its expression was high in ER-negative breast cancer cell lines (MDA- MB- 231, BT-474, MX-1) (Fig.-14, D).

Further, we analyzed whether the STING-IFN pathway is intact in breast cancer cell lines.MCF-7 cells (cGAS +ve/ STING –ve) and MDA-MB-231 (cGAS +ve/STING+ve) were treated with c-di-AMP and monitored the activation of both NF-kB and IFN pathways using luciferase assay. Interestingly c-di-AMP showed no activation of both NF-kB and IFN pathways in MCF-7 whereas it activated both pathways in MDA-MB-231 cells (Fig.-14, E, F). In further experiments, we selected MDA-MB-231 as STING positive cell line and MCF-7 as STING negative cell line. This further suggests that the STING pathway is intact in MDA-MB-231(cGAS +ve/STING+ve) and is inhibited in MCF-7 cells (cGAS +ve/ STING –ve) by downregulation of STING.

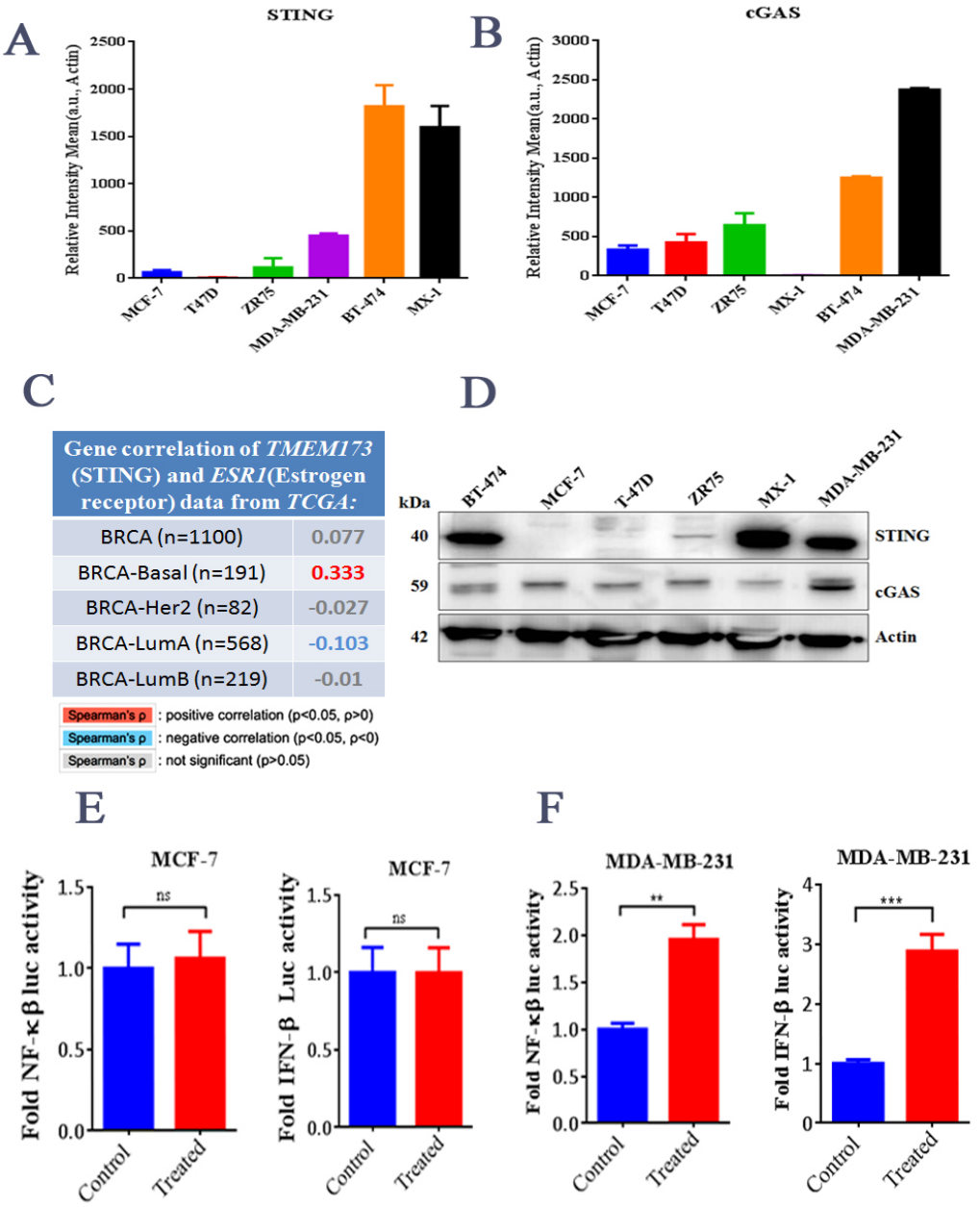

Figure 14 c-di-AMP induces STING-mediated IFN response in breast cancer cell lines

(A) Relative expression of STING in ER-positive (MCF-7, ZR75, T-47D) and ER-negative breast cancer cell lines(BT-474, MX-1 MDA-MB-231)(B)Relative expression of cGAS in ER-positive(MCF-7, ZR75, T-47D) and ER-negative breast cancer cell lines(BT-474, MX-1 MDA- MB-231) (C) Pearson correlation (r) between TMEM173 and ESR1 Data from TCGA (D) Western blot analysis of CAS and STING proteins in breast cancer cell

*lines(E)(F)MCF-7 (STING (–ve)), MDA-MB-231 (STING (+ve))breast cancer cell lines were transfected with IFN-β andNF-κB reporter constructs and treated with c-di-AMP (200μM) for 24 hrs and IFN-β and NF-κB activity was measured. Data represent mean fold change compared to control (n=3Mean ± SD); *P < 0.05, **P < 0.01, and ***P < 0.001, based on a student's t-test.*

4.3.2 c-di-AMP binds to STING

As c-GAMP is known to bind to STING hence we hypothesized its analog c-di-AMP may also bind to STING expressed in human cells. To understand the binding of c-di-AMP as compared to other dinucleotides with STING, we performed docking of c-di-AMP with STING. The pyrimidine ring of purine forms the two hydrogen bonds with Arg238 of STING. The amino group on the pyrimidine ring forms the hydrogen bond with Val239 which is bridged through the conserved water molecule to Ser241 and the oxygen of the phosphate group forms the hydrogen bond and salt bridge with Arg238. The further amino group on the pyrimidine ring of purine forms a hydrogen bond with Tyr 167 and Ser 241. The oxygen of phosphate forms the hydrogen bond with Arg238. The imidazole ring of purine shows the pi-pi interaction with Tyr167and the oxygen atom of phosphate forms the hydrogen bond with Arg238. Interestingly, the purine ring of c-di-GMP shows the pi-pi interaction with Tyr167, and the oxygen atom of phosphate forms the hydrogen bond with Ser162. In di-nucleotide, the amino group on the pyrimidine ring of purine forms a hydrogen bond with Ser241 same as molecule c-di-AMP. The conserved water molecule forms a hydrogen bond with Ser241 and Val239 and oxygen atoms of phosphate form two hydrogen bonds and a salt bridge with Arg238. Apart from these interactions, the molecules also have hydrophobic interactions with Tyr167, Tyr240, Val239, Tyr163, and Leu159 similar to the bound ligand (Fig.-15, A, B, C, D). The docking score of c-di-AMP and c-di-GMP was found comparable and near to the docking score of the co-crystal ligand.

Further, we used cellular thermal shift assay which measures the thermal stability of a target protein and the binding of a ligand to the protein causes an increase in protein melting temperature, hence a quantitative measure of the binding of a ligand. The natural ligand 2, 3'-cGAMP synthesized by cGAS binds to STING and stabilizes it as reported previously[238]. We used a similar method to detect c-di-AMP binding to STING. We

observed that the binding of c-di-AMP stabilized STING protein with increasing temperature whereas unbound STING denatured fast (Fig.-15, F) suggesting the binding of c-di-AMP to STING.

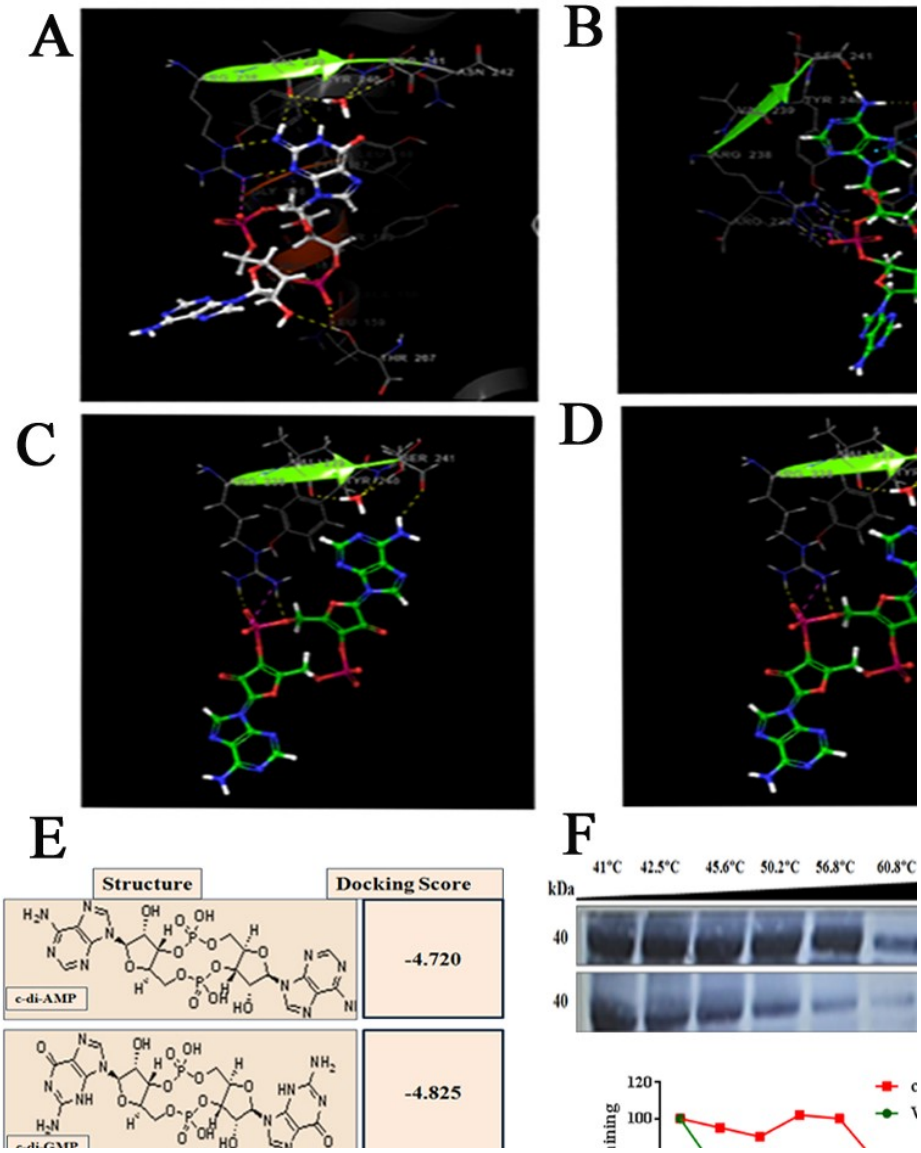

Figure 15 c-di-AMP binds to STING directly

(A) Protein (PDB: 4KSY). Protein (STING) is represented in the wire model and ligands(c-di-AMP) are shown in a ball and stick model where the color represents atoms (Carbon-green, Nitrogen-blue, Oxygen-red, Hydrogen-white, Phosphorus-pink). The dotted lines indicate the protein-ligand interactions (Yellow- hydrogen bond, Pink- salt bridge, Blue- pi-pi interaction) (B)(C)(D) shows the ligand interactions of molecules A, B,

and C with the protein (PDB: 4KSY) respectively. Protein is represented in the wire model and ligands are shown in the ball and stick model where the color represents atoms (Carbon-green, Nitrogen-blue, Oxygen-red, Hydrogen-white, Phosphorus-pink). The dotted lines indicate the protein-ligand interactions (Yellow- hydrogen bond, Pink- salt bridge, Blue- pi-pi interaction) (E) Respective dinucleotide and their Docking score (F)Cellular thermal Shift assay was performed using MDA-MB-231 lysate incubated with c-di-AMP and western blotting was performed.

4.3.3 c-di- AMP activates cell death in ER/PR negative breast cancer cell lines

We and others have previously reported that STING can act as a tumor suppressor by sensitizing the cells to TNF-α induced cell death pathway [218]. We assessed whether c-di-AMP can activate the STING pathway and induce cell death in breast cancer cells. MCF-7 (ER-positive) breast cancer cell line, having an undetectable expression of STING, treated with c-di-AMP showed no effect on cell survival and caspase 3/7 activity (Fig-3, A). MX-1, BT-474, MDA- MB- 231 (ER-negative), STING positive breast cancer cell lines showed a significant decrease in cell survival and increased caspase 3/7 activity (Fig.-16 B, C, D). We analyzed if c-di-AMP can activate apoptotic cell death in breast cancer cells by monitoring PARP cleavage by western blotting. The band of 89 kDa corresponding to the cleaved subunit of PARP was observed in MDA-MB-231 and MX-1 cells whereas no band was detected in MCF-7 cells (Fig.-16, E). The representative images of the fourth day after treatment of c-di-AMP (Fig.-16, F) suggest that c-di-AMP inhibits the proliferation of STING-positive tumor cells and induces apoptosis.

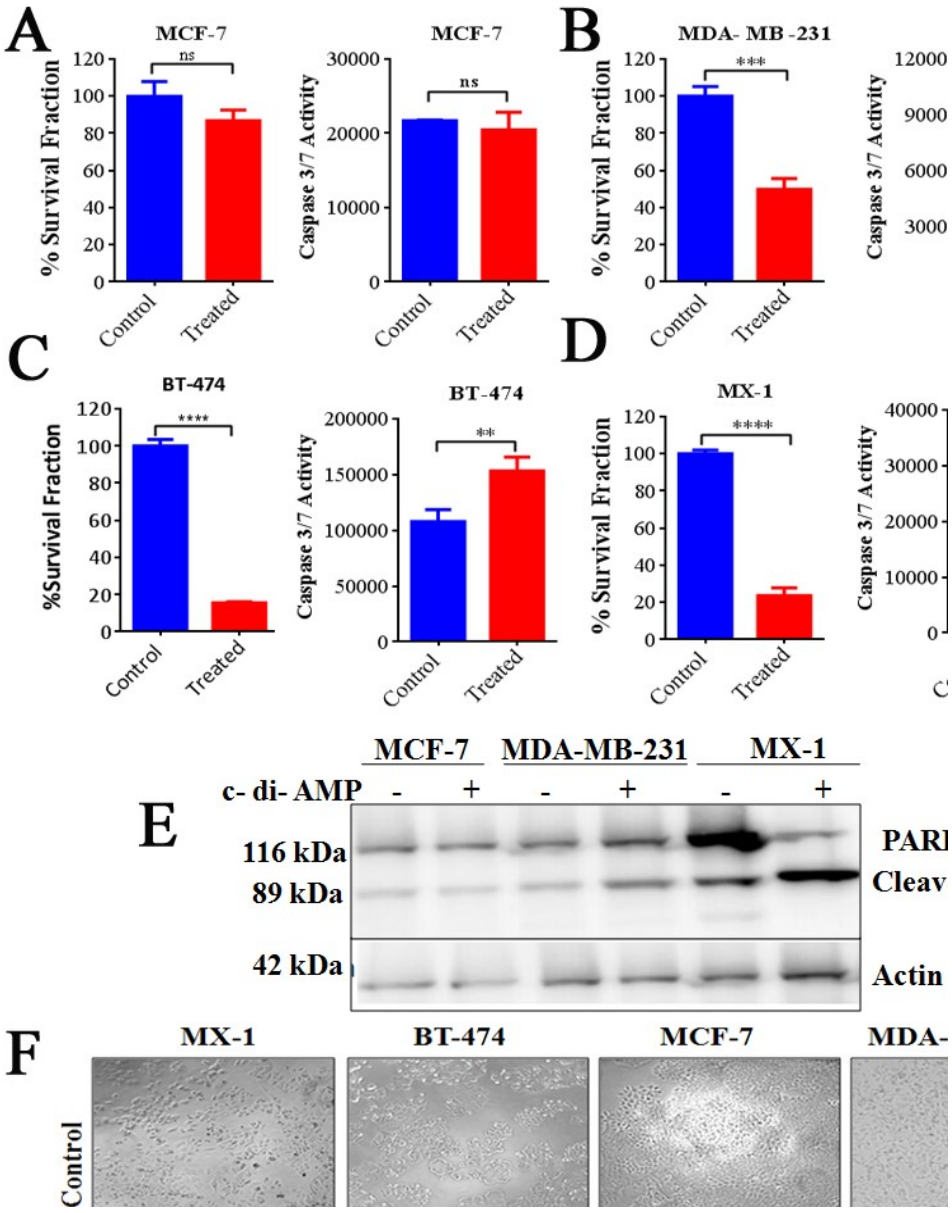

Figure 16 c-di- AMP activates cell death in ER-negative breast cancer cell lines

*Breast cancer cell lines treated with c-di-AMP (200μM) and cell survival was monitored by cell viability assay andCaspase3/7 activity (n=3, Mean ±SD)(A): MCF-7, (B): MDA-MB-231, (C): MX-1; (D); BT-474 n=3, Mean ±SD)(E)MCF-7, MDA-MB-231, MX-1 treated with c- di- AMP (200μM)for 24 hrs and PARP cleavage was analysed by western blotting(F) MCF-7, BT-474, MDA-MB-231, and MX-1 treated with 200μM c-di-AMP and analysed by phase contrast microscopy image captured on the fourth day.*P < 0.05, **P < 0.01 ,***P < 0.001 and ***P < 0.0001 based on a Student's t test.*

4.3.4 STING is essential for c-di-AMP induced cell death

As we observed here that c-di-AMP inhibited cell proliferation, we further characterized the role of STING in the initiation of the cell death pathway. STING was knockdown using shRNA in MDA-MB-231 and BT-474. After the knockdown of STING, cells were treated with c-di-AMP and monitored cellular viability caspase 3/7 activity. We observed that c-di-AMP treatment showed a significant reduction in cell viability in MDA-MB-231 and BT-474 cells, (Fig.-17 A, D) which was rescued after STING knockdown both in MDA-MB-231 and BT-474 cells. Similarly, the caspase-3/7 activity increased significantly in c-di-AMP-treated MDA-MB-231 cells and BT-474 cells (Fig.-17 B, E).The knockdown of STING in MDA-MB-231 and BT-474 rescued cell proliferation and Caspase-3/7 activity of both the cell types. The knockdown of STING (Fig.-17 C, F) was confirmed by western blotting. These experiments strongly suggest that STING is essential for c-di-AMP-mediated cell death in MDA-MB-231 and BT-474 cells.

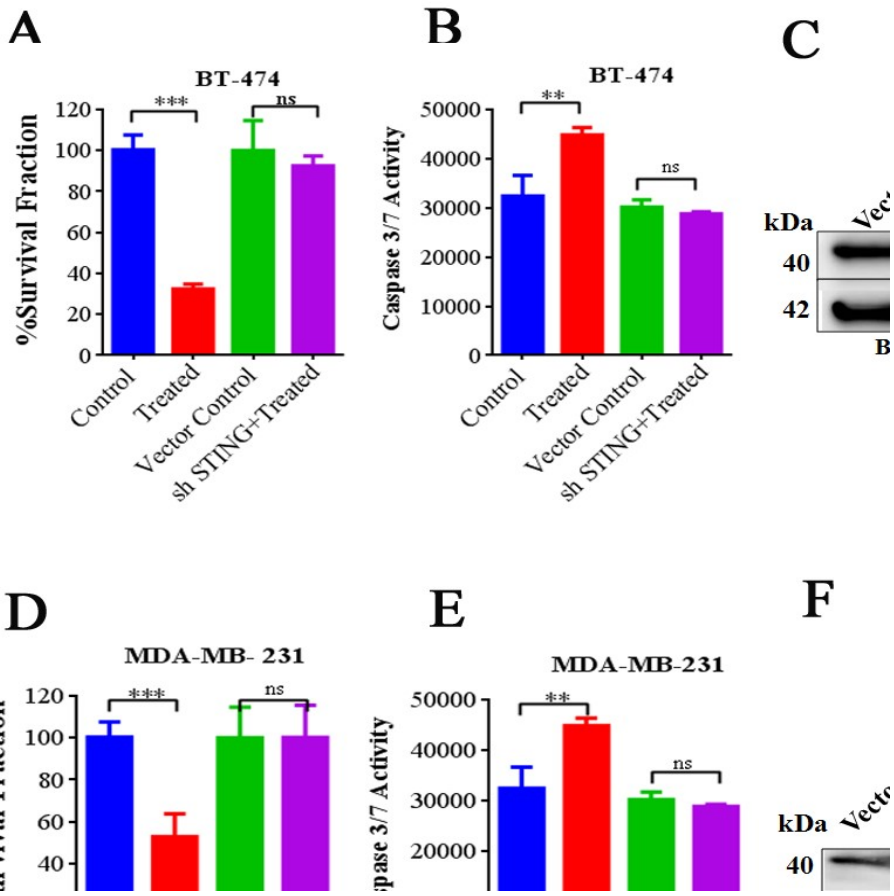

Figure 17 STING is essential for c-di-AMP induced cell death

*(A)(D) BT-474and MDA-MB-231 were transfected with STING shRNA and treated with c-di -AMP (200μM)for 4 days and cell survival was analyzed (n=3, Mean ±SD) (B)(E) BT-474 and MDA-MB-231 were transfected with STING shRNA and treated with 200μM c-di-AMP for 24hrs and Caspase 3/7 activity was measured (n=3, Mean ±SD)(C)(F) Western blot was performed to show the level of STING knockdown in BT-474 and MDA-MB-231 breast cancer cell lines.*P < 0.05, **P < 0.01 and ***P < 0.001, based on a Student's t test.*

4.3.5 IRF-3 is indispensable for c-di-AMP-induced apoptosis in ER-negative breast cancer cells.

The implication of c-di-AMP-regulated NF-κB and IFN pathways for the induction of cell death in breast cancer cells is not understood hence we explored the implication of these pathways in cell death. MDA-MB-231 and MX-1 cells were transfected with p65 and IRF-3 shRNA to inhibit NF-kB and IFN pathways respectively. cGAS, p65, and IRF-3 were knocked out using CRISPR/Cas-9 sgRNA /shRNA, and their role in the regulation of cell death was monitored. The knockdown of cGAS, p65, and IRF-3 was confirmed by western blotting (Fig.-18, A, B). The knockdown of p65 showed no significant change in cell death both in c-di-AMP treated MDA-MB-231 and MX1. Interestingly, the knockdown of IRF-3 significantly enhanced the cell survival in c-di-AMP-treated MDA-MB-231 and MX-1 cells as observed (Fig.-18 C, D). Similarly, IRF-3 knockdown also inhibited caspase activity in c-di-AMP-treated MDA-MB-231 and MX-1 cells (Fig.-18, E, F). We also analyzed the role of cGAS in the regulation of cell death, hence we knockdown cGAS and monitored cell death. The knockdown of cGAS in both cell lines showed no significant change in c-di-AMP-induced cell death suggesting that cGAS acts upstream and is dispensable. These results suggest that IRF-3 is indispensable for c-di-AMP-induced STING-mediated apoptosis in triple-negative breast cancer cells.

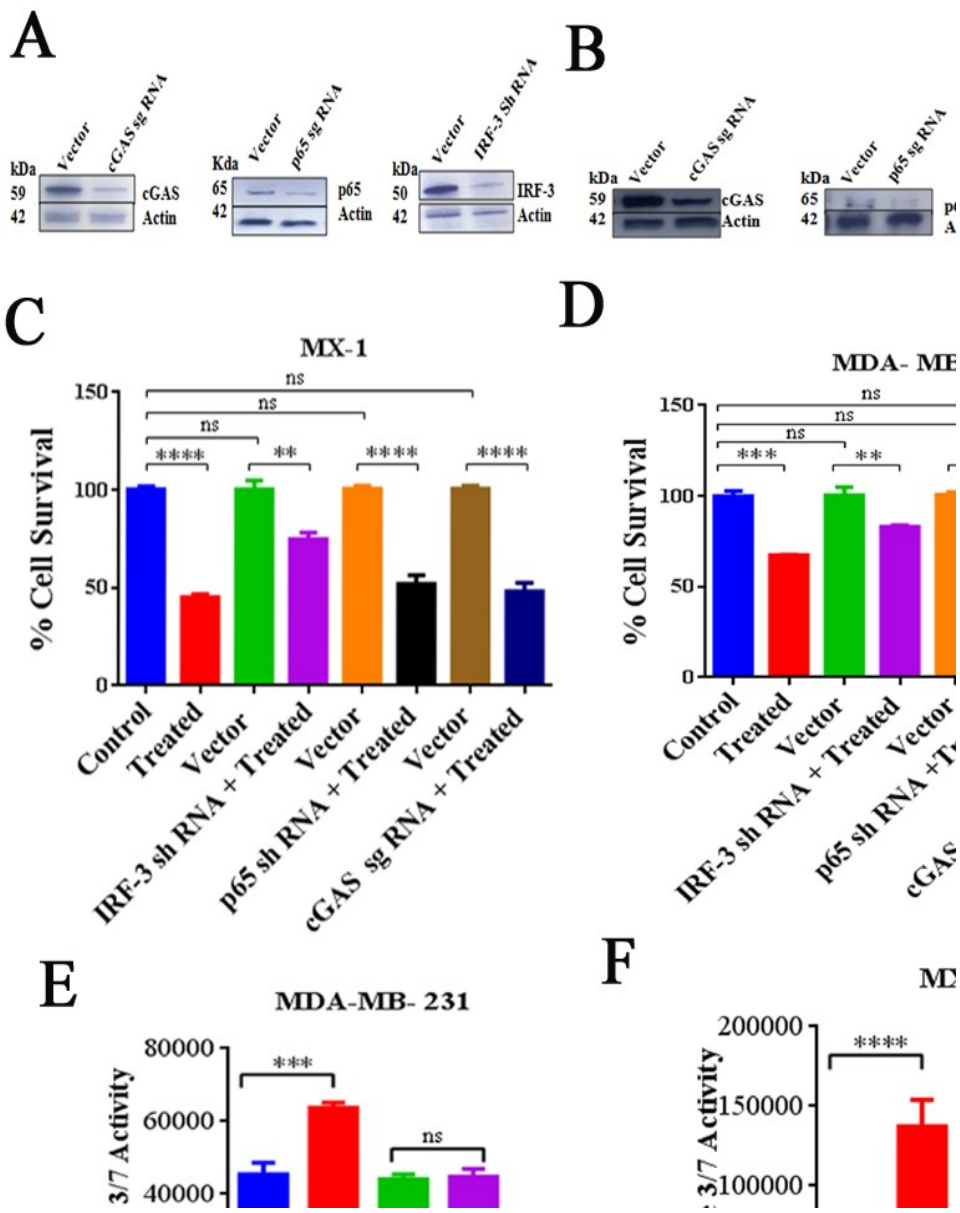

Figure 18 c-di-AMP induces IRF-3 mediated apoptosis in STING-positive, ER-negative breast cancer cells

cGAS, p65 and IRF-3were knockdown MDA- MB- 231 (A) and MX-1 (B) breast cell lines and were treated with c-di-AMP (200μM) and cell viability measured by presto blue(n=3, Mean ±SD), Western blot shows the level of GAS, p65 and IRF-3knockdown in MDA-MB-231 (C) and MX1 (D). cGAS, p65 and IRF-3 knockdown MDA-MB-231 and MX-1 were knockdowns in breast cell line are treated with c-di-AMP 200μM and caspase 3/7 activity

*measured (n=3, Mean ±SD) (E)MDA- MB-231 (F) MX-1cells were knockdown with IRF-3 and treated with c-di-AMP (200μM) after24 hrs capse3/7 activity measured *P < 0.05, **P < 0.01 and ***P < 0.001, based on a Student's t-test.*

4.3.6 c-di-AMP induces IRF-3 translocation to mitochondria and induces the mitochondrial-mediated intrinsic pathway of apoptosis

The above experiment strongly suggests the indispensable role of IRF-3 in c-di-AMP-induced cell death in STING-positive MDA-MB-231 and MX-1 cells. It had been observed previously that IRF-3 activates mitochondrial-mediated apoptosis in virally infected cells [239]. IRF-3 plays a critical role in STING-mediated apoptosis via mitochondrial cytochrome c release [240]. We also monitored the subcellular localization of IRF3-GFP both in MCF-7 and MDA-MB-231 in the presence/absence of c-di-AMP. IRF-3-GFP showed diffused cytoplasmic localization both in MCF-7 and MDA-MB-231. Interestingly c-di-AMP treated cells show distinct puncta of IRF-3-GFP 3 both in MX-1 and MDA-MB-231 cells. The increased numbers of IRF-3 puncta in IRF-3-GFP positive cells were observed in the presence of c-di-AMP as compared to untreated in both MDA-MB-231 cells and MX-1(Fig.-19, A). The co-localization of IRF-3 at mitochondria was checked by co-expressing IRF-3-GFP and mt-RFP constructs in MDA-MB-231 cells. Colocalization was measured by fluorescence microscopy in the presence and absence of c-di-AMP. We observed that the localization of IRF-3 to mitochondria was significantly increased in the c-di-AMP treatment condition in MDA-MB-231 cells (Fig.-19, B).

Hence, we further analyzed if c-di-AMP induces mitochondrial-mediated apoptosis in by measuring PARP cleavage and caspase-9 activation (Fig.-19, C) Treatment of MDA-MB-231 and MX-1 cells with c-di-AMP cells showed the band of 89 kDa corresponding to a cleaved subunit of PARP predominantly in both cells whereas it was not observed in untreated cells. Further, we monitored the cleavage of Caspase-3 in similar conditions. The cleaved subunit of 17 kDa subunit was predominantly observed in c-di-AMP treated both MDA-MB-231 cells and MX1 cells (Fig.-19, D). This was further confirmed by increased caspase 3/7 green fluorescence activity in both cells showing enhanced apoptotic cell death. (Fig.-19, E).Caspase-9 is activated upstream of executioner Caspase-3. Interestingly the cleaved subunit of 35 and 37 kDa was observed in c-di-AMP treated both MDA-MB-231 cells and MX1 cells. To further monitor the effect of c-di-AMP on the clonogenic ability of both MDA-MB-231 and MX-1 cells we performed a colony-forming

assay in presence of c-di-AMP. The clonogenic ability of both MDA-MB-231 and MX-1cells significantly decreased in presence of c-di-AMP (Fig.-19, F). Overall, these results show that c-di-AMP enhances IRF-3 translocation to mitochondria and induces a mitochondrial-mediated intrinsic pathway of apoptosis, inhibiting the clonogenic ability of STING-positive breast cancer cells.

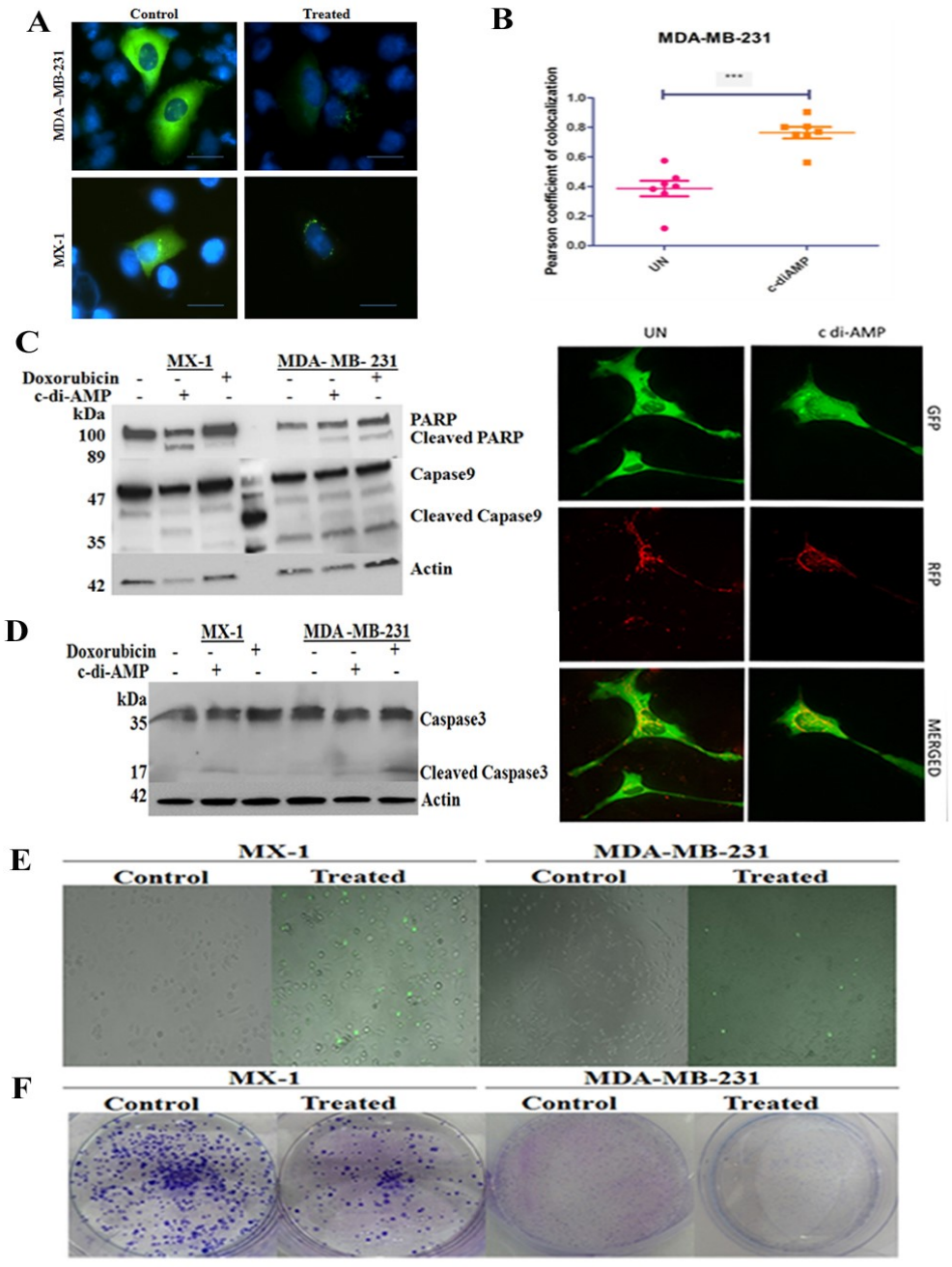

Figure 19 c-di-AMP activates STING-mediated mitochondrial apoptosis

(A) MDA-MB-231 and MX-1 STING expressing cell lines treated with c-di-AMP 200μM for 24 hrs and IRF-3 puncta was measured using a fluorescence microscope (B) MDA-MB-231 cells were overexpressed with IRF-GFP and mt-RFP constructs and their colocalization was measured using fluorescent microscopy in presence and absence of c-di-AMP (C)&(D)Western blotting was performed in MDA-MB-231 and MX-1 STING expressing cell lines by treating with c-di-AMP 200μM after 24 hrs to measure cleaved PARP, Caspase 9 and cleaved caspase3 (E) STING expressing cell lines MDA-MB-231 and MX-1 were treated with c-di-AMP (200μM) for 24 hrs and caspase/7 green activity was measured using microscopy(F) MDA-MB-231 and MX-1 cells were treated with 200μM c-di-AMP and the colony-forming assay was performed

4.3.7 Discussion:

Highly proliferating tumor cells show a high level of chromosomal instability which has becomes the hallmark of cancers of different origins [241]. The reports from our previous lab and others had shown that ER-positive breast cancer cells are STING-negative and the Gene expression correlation between *TMEM173* (STING) and *ESR1*(Estrogen receptor) also reflect the same like all types of breast cancer STING expression and Estrogen receptor negatively correlates except a basal type of breast cancer this suggest that ER expressing breast cancer having a low expression of STING [230]. whereas highly proliferative cells ER/PR/Her-2 negative, MDA-MB-231 and MX1 cells, are STING positive [218]. It has been observed that chromosomal instability promotes errors in chromosome segregation which leads to micronuclei formation and leakage of genomic DNA into the cytosol[26][242]. This leads to the activation of the cGAS–STING cytosolic DNA-sensing pathway and downstream noncanonical NF-κB [243]. signaling leading to proliferation and metastasis. Cyclic dinucleotide, cGAMP, is an endogenous high-affinity ligand for the adaptor protein STING [244]. The synthesis of the cGAMP analog like c-di-AMP in bacteria is an interesting phenomenon and modulates the STING pathway during infection however its potential in regulating these pathways and modulation of cell death in breast cancer cells has not been well studied. We observed that c-di-AMP can activate apoptosis in ER-negative breast cancer cells modulation of cell death in breast cancer cells has not been well studied.

We observed that c-di-AMP can activate NF-κB and IFN pathways in breast cancer cells depending upon the presence of STING. It was observed that ER-positive cells are low STING or negative expressing cells and ER-negative cells show high STING positivity. The evidence here suggests that STING is eliminated or down-regulated during the early stage of the growth hormone ER/PR positive cells where some cells retained STING and became growth hormone-independent[245]. This supports the emerging hypothesis of clonal evolution of the cells which positively determines tumor growth and metastasis by clonal amplification and retaining the gene expression at the different stages of cancer. Basal STING activation is essential for cell proliferation and metastasis by promoting non-canonical activation of NF-kB [54]. This hypothesis is in consonance with earlier reports where STING-positive cells showed enhanced proliferation, brain metastasis cells, and chemoresistance in breast cancer cells and lung cancer cells. Previously it had been observed that cGAMP can be transferred from the metastatic cells to brain astrocytes through cellular GAP junctions [243]. The intactness of the type-I IFN pathway and NF-kB may play an essential role in tumor cells which can be therapeutically targeted. Further c-di-AMP can activate NF-kB and IFN in triple-negative breast cancer cells suggesting that the STING pathway is intact as compared to ER/PR-positive breast cancer cells. STING-NF-kB and/IRF-3 pathway is intact in triple-negative breast cancer as compared to ER/PR-positive cells as observed in this study and can be differentially modulated by c-di-AMP. This is an interesting characteristic of aggressive breast cancer cells which can be further investigated and can be exploited therapeutically.

Interestingly sustained activation of the STING pathway by c-di-AMP shows the activation of cell death specifically in ER/PR negative cells and not in ER-positive cells where the IRF-3 pathway seems to be essential for the cell death pathway. Interestingly, c-di-AMP is induced translocation of IRF-3 to mitochondria and activation of mitochondrial pathway in ER-negative cells which aligns with the earlier observation of IRF-3 translocation to mitochondria during viral infection-induced apoptosis[246]. This pathway is although independent of the DNA binding ability and is dependent upon mitochondrial localization [247].We also observed that mitochondrial functions are compromised leading to the activation of Caspase-9 mediated Caspase-3 activation in MDA-MB-231 cells and MX1 cells. This pathway is not activated in MCF-7 and other ER-positive cells. MCF-7 is also IRF-3 positive cells however ER/PR positive cells are either less/negative STING,

this suggests that a critical level of STING is required for c-di-AMP-induced cell death in breast cancer cells. The sustained activation of STING-mediated pathways with fewer side effects is a requirement that may activate the immunogenic cell death pathway[151] specifically in triple-negative breast cancer cells which are highly proliferative and metastatic and show high-level chromosomal instability. It had been observed previously due to chronotherapies and the formation of miro nucleoli there is a release of DNA leading to cGAS/cGAMP/STING activation however no IFN activation[50]. However, release of DNA leads to activation of the non-canonical NF-kB pathway which may be determined by the strength of cGAMP-induced signaling and which is enzymatically regulated and determine the outcome. Therefore, the sustained activation of this pathway by cGAMP analog-like c-di-AMP may induce IR3 translocation to mitochondria and induce intrinsic pathway of apoptosis. There is no direct comparison of cGAMP with CDNs however isolated studies suggest cGAMP rather than therapeutic beneficial it may further support growth [248][243].

This study provides a rationale for screening the bacterial-origin cyclic dinucleotides which may activate the intrinsic cell death pathway and may activate the immunogenic cell death pathway. Therefore, the bacterial-derived c-di-AMP and other analogues should be screened for their potential as combinatorial therapy with DNA damaging agents for therapeutic potential in breast cancer cell lines and patient-derived xenograft model. Previously, the potential of c-di-GAMP increased the expression levels of maturation markers CD80/CD86 and MHC-II on DCs isolated from spleens of 4T1 tumor-bearing mice, which is important for the presentation of tumor-associated antigens (TAAs) and activation of TAA-specific T cells and can cause tumor regression. The potential of c-di-AMP and other bacterial-derived di-nucleotide and human-origin di-nucleotide should be explored for the potential in antigen presentation and tumor cell-intrinsic cell death mechanism and should be exploited for therapeutic potential.

4.4 Activation of cGAS and anti-cancer therapy

4.4.1 $MnCl_2$ activates STING-mediated IFN response

Mn^{2+} is a trace inorganic nutritional element required for various biological processes including development, reproduction, neuronal functions, and oxygen defences[249]. Mn^{2+} also plays a role as a cofactor for some enzymes like metalloenzymes like Mn^{2+} superoxide dismutase, glutaminesynthase, and arginase[250]. Largely role of Mn^{2+} is not very well understood but a recent study shows that Mn^{2+} was essential as a co-factor for cGAS and activates its enzymatic activity after the detection of cytoplasmic dsDNA[251]. Mn^{2+} can also activate catalytic activity cGAS and generate 2'3' cGAMP even in absence of infection and cytoplasmic dsDNA[252]. This strongly suggests that Mn^{2+} is an indirect agonist for STING and hence has the potential of enhancing the efficacy of immune therapy against cancer[179]. The role of different metals and activation of type-1 IFN response in breast cancer is not understood hence we explored the role of different metal ion mediated activation of the type-1 IFN response in breast cancer cell line. MDA-MB-231(cGAS +ve) and STING(+ve) cells were treated with a different metal ion ($MnCl_2$, $MgCl_2$, $CoCl_2$, $FeCl_2$) with different concentrations and monitored IFN-β activation using luciferase assay. The metal ions like Fe, Co and Mg showed no effect on IFN activation. Interestingly, $MnCl_2$ induced IFN-β in a dose-dependent manner (Fig.-20, A). Further, we selected $MnCl_2$and explored its potential as a stimulator of the cGAS STING pathway in breast cancer cell lines. Hence, we used MDA-MB-231 as (STING +ve) and (cGAS +ve) cells and MCF-7 as (STING –ve) and (cGAS +ve) cells. We treated cells with different concentrations of $MnCl_2$and monitored activation of IFN-β pathway using luciferase assay. Interestingly $MnCl_2$ showed no effect on luciferase activity in MCF-7. However enhanced MDA-MB-231 show dose-dependent induction of IFN-β luciferase activity (Fig.-20, B, C).

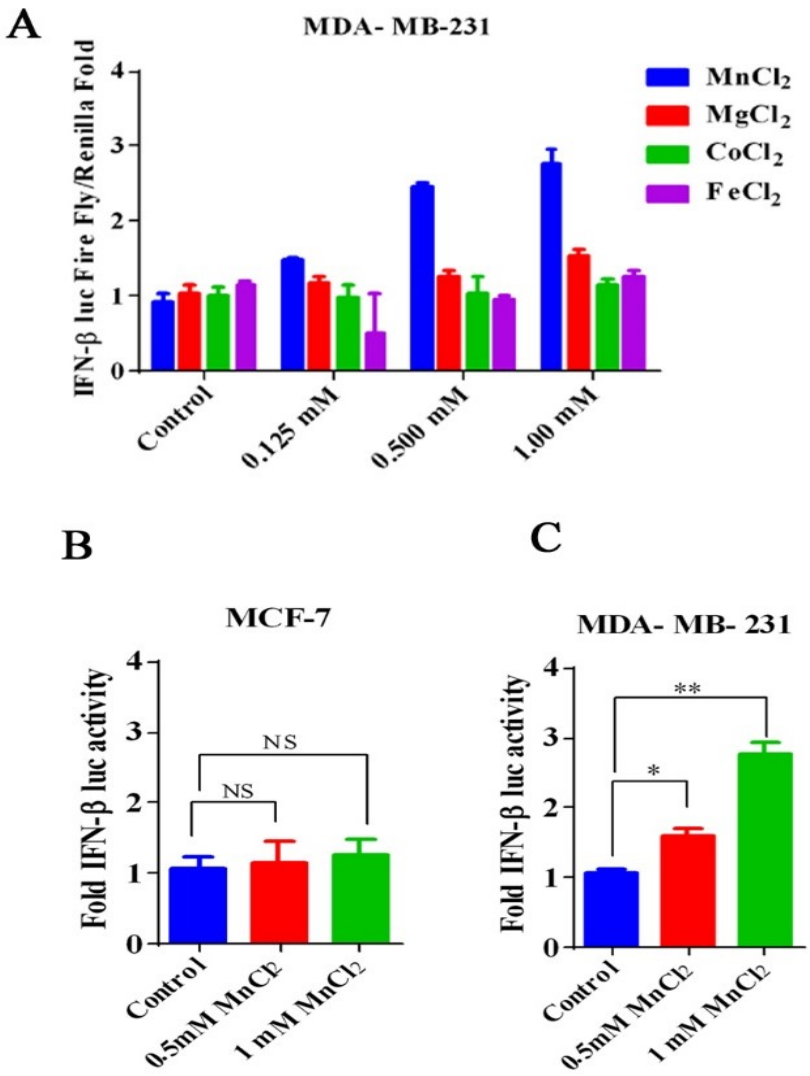

Figure 20 $MnCl_2$ activates STING-mediated IFN response

MDA-MB-231 [cGAS(+ve), STING (+ve)] breast cancer cell line was transfected with IFN-β Luc reporter constructs and treated with different concentrations of metal ions for 24 h and IFN-β activity was measured. Data represent mean fold change compared to control (n=3, mean ± SD) (A). MCF-7 [cGAS (+ve), STING (–ve)], MDA-MB-231 [cGAS(+ve), STING (+ve)] breast cancer cell lines were transfected with IFN-β Luc reporter constructs and treated with different concentration of $MnCl_2$ for 24 h and IFN-β luciferase activity was measured. Data represent mean fold change compared to control (n=3, mean ± SD).

4.4.2 cGAS and STING are indispensable for $MnCl_2$-mediated IFN activation in breast cancer cells

It has been reported that during viral infection Mn^{+2} is released from different cellular organelles and sensitizes cGAS to cytoplasmic DNA and enhances its enzymatic activity [251]. We analyzed the role of cGAS and STING in Mn^{+2} activated in the IFN-β pathway. We selected the MDA-MB-231 cell line as [cGAS(+ve), STING (+ve)] and co-transfected sequentially shRNA STING and sgRNA cGAS with IFN-β Luc construct and treated with different concentrations of $MnCl_2$, IFN-β activity was measured using luciferase assay. Interestingly, the knockdown of cGAS and STING inhibited the activation of IFN-in the presence of $MnCl_2$ (Fig.-21 A, B). The knockdown protein western blot as knockdown of cGAS and STING in MDA-MB-231(Fig.-21 C, D) was confirmed by western blotting.

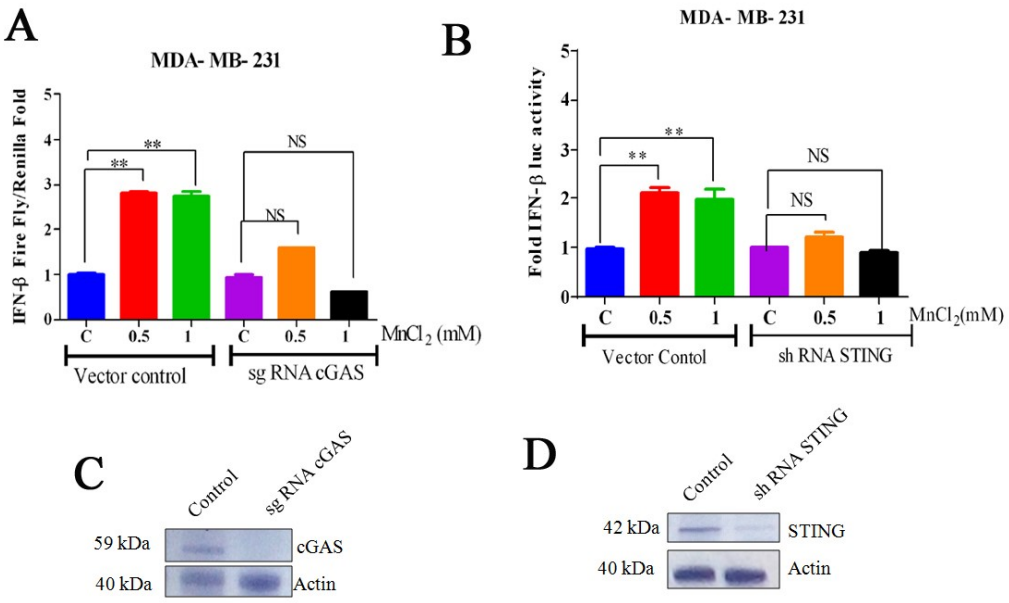

Figure 21 cGAS and STING are indispensable for $MnCl_2$-mediated IFN activation in breast cancer cells

Effect of cGAS and STING knockdown on IFN-β activation: Sequentially cGAS and STING knockdown in MDA-MB-231, cells were transfected with IFN-β Luc and treated with different concentrations of $MnCl_2$ for 24 h, and luciferase activity was analyzed using DLR assay, Data represent mean fold change compared to control (n=3, mean ±SD) (A)(B) and representative knockdown western blot for cGAS and STING (C)(D).

4.4.3 $MnCl_2$ sensitizes breast cancer cells to paclitaxel-induced cell death:

Paclitaxel is a widely used drug for the treatment of cancer including breast cancer [253]. It has been reported that patients who received paclitaxel treatment have high infiltration of lymphocytes in the tumoral stroma. During the paclitaxel treatment, a micronucleus is formed and a cytoplasmic micronucleus is accessible to cGAS and recruits STING to activate the downstream IFN pathway[254]. Type-1 interferon synthesized during the paclitaxel treatment act as pro-apoptotic priming and increased the threshold for induction of apoptosis[255]. As observed here Mn^{2+} enhanced cGAS activity in MDA-MB-231 cells we hypothesized that combinatorial therapy of $MnCl_2$ and Paclitaxel may enhance the anti-tumor response. MDA-MB-231 and MDA-MB-468 TNBC cancer cell lines were treated with different concentrations of Paclitaxel, $MnCl_2$, and in combination, and cell viability was measured. Interestingly combination of both contour plotted and dark blue intensity show synergy in growth inhibition in both the cell lines (Fig.-22, A, B). The combination of paclitaxel and $MnCl_2$ shows significant inhibition of MDA-MB-231 and MDA-MB-468(Fig.-22, C, D) and upregulation of caspase3/7 activity (Fig.-22, E, F) as compared to control and individual treatments.

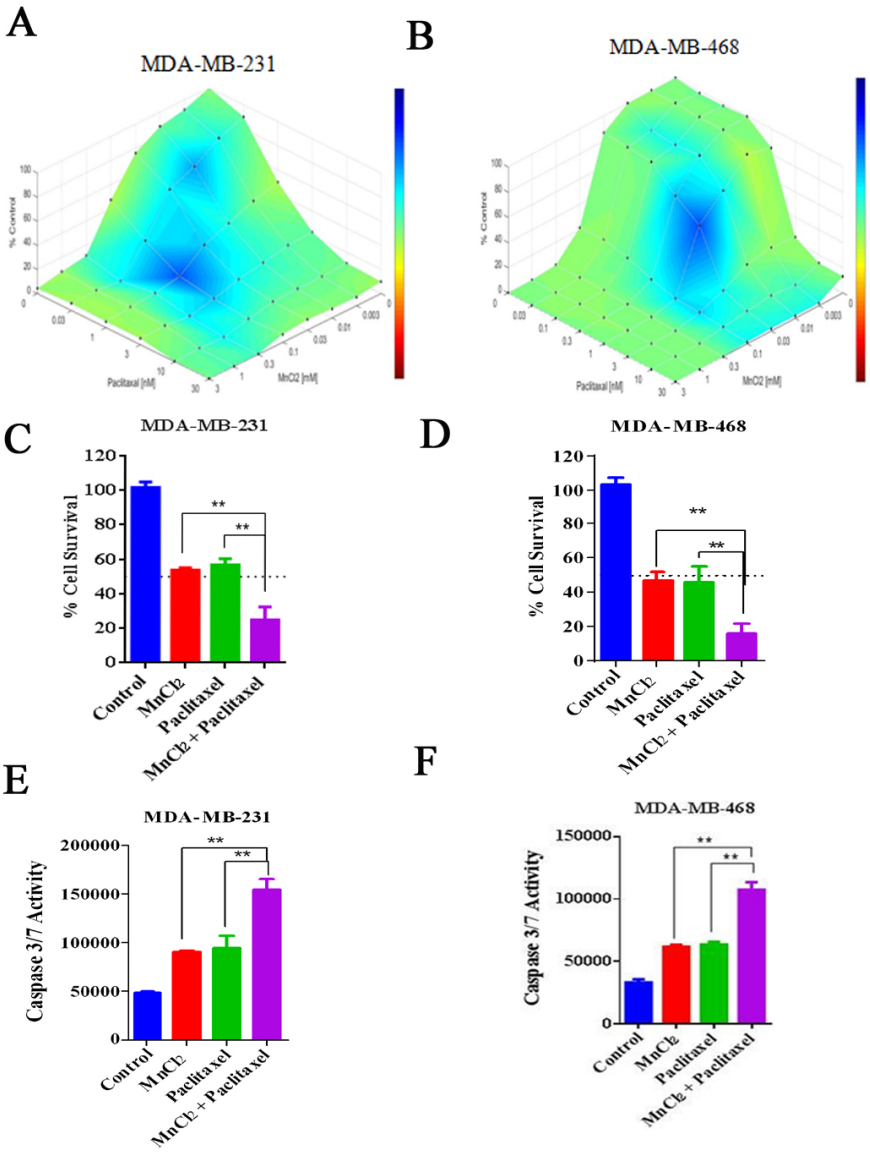

Figure 22 $MnCl_2$ and Paclitaxel act synergistically to induce cell death in triple-negative breast cancer cells

Synergistic potential of $MnCL_2$ and paclitaxel: MDA-MB-231 and MDA-MB-468 treated with different concentration combination matrix and alone and cell viability measured and surface plot of synergy plotted using combenefit Cambridge software(A)(B). Effect of the combinatorial potential of $MnCl_2$ and Paclitaxel on growth inhibition and apoptosis: Cells were treated with alone paclitaxel, $MnCl_2$, and With the combination of both after treatment cell viability measured, data represented mean % cell survival± SD(C, D) and

as described Apoptosis marker has been evaluated using caspase3/7 activity data represented mean RLU ± SD(E, F)

4.4.4 Combination of $MnCl_2$ and Paclitaxel enhanced immunogenic cell death of breast cancer cells.

It had been observed that prolonged mitosis due to inhibition from taxanes induces sufficient activation of the cGAS STING pathway [256].On the other end, $MnCl_2$ sensitized cGAS independent of dsDNA, hence we hypothesized that a combination of paclitaxel and $MnCl_2$ may activate IFN and may activate this pathway above the threshold and may activate the immunogenic cell death. Firstly we monitored if a combination of $MnCl_2$ and paclitaxel can synergistically activate IFN in MDA-MB-231 and MDA-MB-468 cell lines. Cells were transfected with IFN-β Luc construct and treated with different concentrations of $MnCl_2$ and Paclitaxel and combination and monitored luciferase activity. Interestingly combination of both shows profound upregulation of IFN-β activity (Fig.-23, A,B). We further analyzed if combinatorial treatment also activates immunogenic cell death by enhancing T cell activation. We co-cultured MDA-MB-231 and PBMCs with a 1:16 ratio and cells were treated with $MnCl_2$, Paclitaxel and in a combination of both. Interestingly we found the profound killing of MDA-MB-231 in combination treatment. (Fig.-23 , C) and Survuval plot as (Fig.-23,D)

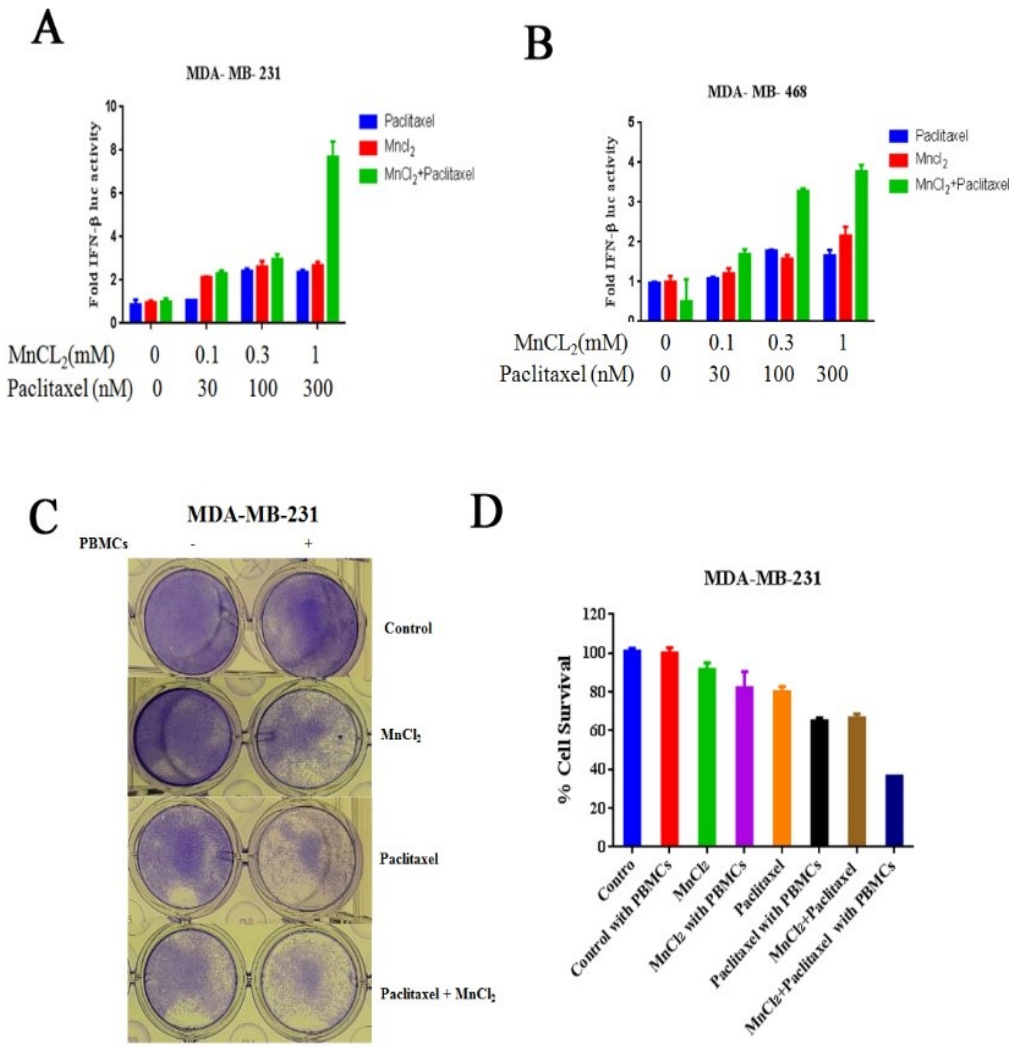

Figure 23 Combination of $MnCl_2$ and paclitaxel enhanced immunogenic cell death of breast cancer cells

$MnCl_2$ add synergy in the activation of IFN during treatment of Paclitaxel: MDA-MB-231 and MDA-MB-468 cell line and transfected with IFN-β luc contract and treated with different concentration of $MnCl_2$ and Paclitaxel or in a combination of both and next day relative luminance measure and data represented with mean fold induction as compared to individual ± SD (A),(B). PBMCs mediated killing of tumor cells: MDA-MB-231 cells treated with $MnCl_2$ and paclitaxel and in combinations with both and co-cultured with PBMCs and incubated for 4 days and cell viability measured and plate well stained with Giemsa representative image(C) cell viability represented as % mean survival ± SD(D)

4.4.5 Discussion:

The understanding of mitosis had led to the development of specific molecules that target different processes of mitosis. Many drugs have been identified that target different processes in mitosis. Taxol had shown success in solid tumors including breast cancer[253]. The high rate of proliferation in malignant cells including TNBC breast cancer cells shows a high rate of chromosomal instability number [50]. These cells show mitosis defects leading to the formation of micronuclei which activate the cGAS/STING pathway leading to inflammation [241]. These tumor cells evolve to selectively amplify oncogene or lose tumor suppressor genes to for tumor growth and modulate the pathway for the survival of tumor cells.

Interestingly breast cancer and other solid tumors showed basal expression of cGAS however retained specific cell types only retained STING. In breast cancer, most of the cell types retained cGAS however only triple-negative breast cancer cells retained STING and show an alternate pathway of the cGAS/STING pathway which enhanced their survival.

This further helps by making the microenvironment cold by suppressing the tumor cells' specific immunogenic cell death and recruitment of the other tumor cells. Metals are important co-factors of cGAS and downstream activation of the STING pathway however the combinatorial potential of $MnCl_2$ with other anti-tumor drugs and their potential in breast cancer has not been well investigated.

It has been observed that taxane specifically, Paclitaxel, persists for a longer period in the solid TME including breast cancer, presumably bound to microtubules, whereas drugs specifically targeting show typical ordinary pharmacology. low period and less specific. Paclitaxel causes chromosome segregation errors and micro-nucleated, which may activate the cGAS/STING pathway. Therefore, lower concentration effects along with a longer period in tumors make it the preferred choice for the therapy. However, it is important to develop the cold tumor microenvironment into a hot and activate immunogenic tumor cell death. Metals are interesting and important for the activation of the immune system. $MnCl_2$ is a co-factor of cGAS and activates downstream STING. The efficacy is not well understood in breast cancer. The evidence here strongly suggests that $MnCl_2$ specifically activates the type-1 interferon in triple-negative breast cancer cells which is STING

positive. This is in consonance with an earlier report of $MnCl_2$ activating the cGAS-STING pathway and innate immune response. The results also here demonstrate that the cGAS-STING pathway is essential for the activation of the type-1 interferon pathway. As reported previously several breast cancer cells are cGAS positive however, STING is lost in ER/PR +ve cells whereas retained in triple-negative breast cancer cells. The retained expression is modulated in an alternate way of STING activation turning TME in cold and immunosuppressive in triple-negative breast cancer cells.

It is important to develop combinatorial therapy to achieve a better therapeutic outcome in three different ways: targeting highly proliferative cells, decreasing the apoptotic threshold, and activating an immune response. We tested the combinatorial potential of $MnCl_2$ and paclitaxel. As mentioned earlier also paclitaxel is interesting and leads to abnormal mitosis. Interestingly cGAS has no effect on the cells where normal mitosis proceeds however cGAS specifically recognizes the cells where they show abnormal mitosis and form micronuclei. Further, cGAS also promotes cell death after mitotic arrest in breast cancer cells.

It was observed that combination of decreased cell viability and enhanced the activation of cell death specifically in STING-positive cells. Further, we also observed that this combination is effectively activating the IFN pathway and hence may have the potential to convert the cold TME to a hot and immune-active environment. The combination activated immunogenic cell death effectively.

Immunosuppressive TME is a major problem in solid tumor immunotherapy. Therefore, the intense focus had been to identify the agonists of the STING pathway to induce type-1 interferon activation and innate immune responses to convert cold into hot TME. STING-targeted monotherapies had been taken up to clinical trials however, tumor resistance to STING is observed. Therefore, alternative approaches need to be further explored. The current study suggests the potential of Mn^{2+} and paclitaxel as effective combinatorial therapy targeting only highly proliferative cells which show more potential for metastasis. This combination needs to be further tested in vivo models and analyzed the activation of immunogenic cell death. Further, this needs to be also tested if this combination can overcome the tumor resistance to STING monotherapies.